Electrical Power and Energy Systems 172 (2025) 111142

Contents lists available at ScienceDirect

International Journal of Electrical Power and Energy Systems

journal homepage: www.elsevier.com/locate/ijepes

Distributed coordination of electric vehicles charging station and home energy management systems in residential neighborhood

Farshad Etedadi [a,*], Abdoul Wahab Danté [b], Sousso Kelouwani [c], Nilson Henao [a], Kodjo Agbossou [a], Michaël Fournier [d]

[a] Department of Electrical and Computer Engineering, Hydrogen Research Institute, University of Quebec at Trois-Rivières, Trois-Rivières, G8Z 4M3, QC, Canada
[b] Hydro-Québec's Research Center (CRHQ), Varennes, J3X 1S1, QC, Canada
[c] Department of Mechanical Engineering, Hydrogen Research Institute, University of Quebec at Trois-Rivières, Trois-Rivières, G8Z 4M3, QC, Canada
[d] Energy Technology Laboratory (LTE), Hydro-Québec's Research Center (CRHQ), Shawinigan, G9N 7N5, QC, Canada

ARTICLE INFO

Keywords:
Demand response
Electric vehicles
Home energy management
Coordination
Transactive energy
Shapley value

ABSTRACT

The uncoordinated management of Electric Vehicle (EV) Charging Station Management Systems (CSMS) and Home Energy Management Systems (HEMSs) has been shown to have detrimental effects on the distribution system, leading to the creation of new demand peaks (rebound) and increased power loss in the grid. This paper develops a distributed coordination approach for managing CSMS and HEMSs agents, aimed at mitigating the negative impacts of uncoordinated consumers within a neighborhood. A comprehensive model of consumer flexibility is developed by integrating residential demands with detailed CSMS features, including EV charging schedules and energy requirements, as well as the impact of temperature on charging duration. The proposed coordination technique not only fulfills individual objectives of agents but also addresses shared objectives of the neighborhood, which are distributed among all agents by a coordinator. The technique aims to harmonize HEMSs and CSMS consumption profiles to smooth out the aggregated profile and reduce the neighborhood's total energy costs. Afterward, an incentive allocation mechanism has been devised to assess the marginal contributions of agents and distribute rewards accordingly. The proposed CSMS and HEMSs coordination is evaluated through case studies encompassing diverse preferences, coordination levels, as well as parameters uncertainties. Additionally, the proposed approach is compared against both the uncoordinated and indirect coordination cases, implemented using proximal dynamic prices. The evaluation demonstrates that, compared to the baseline scenario, the load factor improves significantly by up to 35%, and the total neighborhood discounted bill is reduced by up to 27%.

1. Introduction

1.1. Motivation

In the context of modern energy systems, coordinating Energy Management Systems (EMS) is crucial for integrating residential consumers exploiting Home Energy Management Systems (HEMS), distributed generations, energy storage systems, and electric vehicles (EV) in neighborhood areas of the distribution grid [1]. Coordinated EMSs harness flexibility sources within the neighborhood to tackle local challenges such as rebound peak and contingency, and alleviate stress on the distribution system, all without substantial infrastructure upgrades [2]. The application of coordinated EMS spans various domains: [1,3,4] encompass innovative demand side managements, [5–8] delve into distributed generations, [9,10] focus on EVs charging, and [11,12] explore storage system and power flow.

According to the Canada Energy Regulator report [13], currently, electricity accounts for nearly 43% of the residential energy demand, a figure projected to rise to 76% by 2050. This trend indicates a significant increase in electrification within the residential sector, highlighting the importance of coordinating HEMSs to effectively manage the anticipated surge in electricity demand and alleviate strain on the grid. Besides, a recent study by the International Energy Agency (IEA) forecasts that 64% of global light-duty vehicles will be electric by 2030, with a full 100% electrification expected by 2050 [14]. Uncoordinated EV charging behaviors can lead to demand peaks and increased power loss in the distribution network. Hence, considering the trends in EVs and residential consumption, coordinating HEMSs and EV charging is essential for flattening the aggregate load and optimizing total energy costs bu exploiting users' flexibility.

* Corresponding author.
E-mail address: farshad.etedadi.aliabadi@uqtr.ca (F. Etedadi).

https://doi.org/10.1016/j.ijepes.2025.111142
Received 21 February 2025; Received in revised form 6 August 2025; Accepted 11 September 2025
Available online 3 October 2025

Nomenclature

Acronyms

LF	Load factor
ADMM	Alternating direction method of multipliers
CC	Constant current
CCCV	Constant current - constant voltage
CS	Charging station
CSMS	Charging station management system
CV	Constant voltage
DR	Demand response
DSO	Distribution system operators
EH	Electric heater
EMS	Energy management system
EV	Electric vehicle
EVSE	Electric vehicle supply equipment
HEMS	Home energy management system
PEV	Plug-in electric vehicle
SOC	State of charge
TCM	Transactive coordination mechanism

Parameters

Δt	EV charging optimization time step in hour
$\hat{\eta}^{v}_{c,T}$	Charging efficiency estimate for EV index v considering the ambient temperature T
$\hat{P}^{v}_{\text{av}}$	Average power profile of EV index v in kW
$\text{SOC}^{v}_{\text{desired}}$	Desired state of charge of the EV index v battery at the departure time
$\text{SOC}^{v}_{\text{initial}}$	Initial state of charge of the EV index v battery at the arrival time
p_{Di}	Active power demand at bus i
s^{v}_{h}	Parking status of the EV index v in the charging station at the time index h
α, β, γ	Thermal coefficients
$\mathcal{N}_{\text{EV}}$	Number of electric vehicles in neighborhood
$\mathcal{N}_{\mathcal{H}}$	Number of houses in neighborhood
$\mathcal{N}_{\mathcal{N}}$	Number of neighborhoods
CR	Coordination level
ω	Daily comfort levels profile
θ	Electricity price
$E^{\text{DT}}_{\text{max}}$	Maximum energy capacity of secondary distribution transformer
$E^{\text{NT}}_{\text{max}}$	Maximum energy capacity of neighborhood transformer
E^{H}_{min}, E^{H}_{max}	Minimum and maximum house total energy profile limit
$E^{\text{EH}}_{\text{min}}$, $E^{\text{EH}}_{\text{max}}$	Minimum & maximum EH energy
H	Horizon length
Q^{v}_{cap}	Battery capacity of EV index v in kWh
T^{δ}	Indoor temperatures allowable range
$T^{\text{in}}_{\text{min}}$ and $T^{\text{in}}_{\text{max}}$	Minimum & maximum allowable indoor temperatures
T^{SP}	Desired indoor temperature
T_{out}	Outdoor temperature
$T^{\delta}, P(T^{\delta})$	Indoor temperature allowable range distribution
$T^{\text{SP}}, P(T^{\text{SP}})$	Desired indoor temperature distribution
$\omega_{\text{min}}, \omega_{\text{max}}$	Minimum & maximum comfort levels

Indices

C_G	Grand coalition comprising all agents
s	EV charging session index
v	EV index
h	Time-slot
$\mathbb{RG}_l, \mathbb{RG}_m$	Residential groups set l & m
$\mathbb{S}_f, \mathbb{S}_g$	Societies set f & g
i	House's index
k	Iteration's index
RG	Residential group

Sets

$\mathcal{T}$	Set of time step space for optimization
$\mathcal{V}$	Set of all EV in the neighborhood coordination scheme
Ω	Comfort set
$\mathbb{C}$	Set of all possible agent coalitions
$\mathcal{H}$	Horizon set

Variables and Functions

u^{v}_{h}	Binary control variable representing the vth EV charging decision (ON/OFF) at the time slot h from the CSMS
x^{v}_{h}	Accumulated energy charged to the EV battery indexed by v from the plug-in time to the time index h.
x^{CC}_{s}	EV energy requirement in CC phase
x^{CV}_{s}	EV energy requirement in CV phase
$\bar{Z}$	Global variables averaged (ADMM)
λ	Dual variables (ADMM)
$\mathcal{W}(C)$	Worth of coalition C (known as value function)
$\Psi_i(\mathcal{W})$	Agents shares (Shapley values)
SOC^{v}_{h}	State of charge of the battery of the EV index v at time slot h
$E^{\text{CR}}_{C_G}$	Energy profile of grand coalition C when there is coordination
$E^{\text{NCR}}_{C_G}$	Energy profile of grand coalition C when there is no coordination
E^{CR}_{C}	Energy profile when in sub coalition C there is coordination
E^{NCR}_{C}	Energy profile of sub coalition C when there is no coordination
T^{in}	Indoor temperature
J^{H}_{i}	Individual cost function of house i
J^{CS}	Individual cost function of charging station
Z	Global variables averaged (ADMM)
E^{CS}	Charging station total energy consumption
E^{EH}	Electric heater energy usage
E^{FL}	House fixed load demand
E^{H}	Household total energy consumption

1.2. Related works

It is crucial to delineate multi-agent coordination approaches from other valuable but distinct contributions within the broader energy management literature. Notably, some research focuses on energy management and control for individual entities, such as a EV station [15] or a smart home integrating assets such as local generation and EV [16–

18]. Other works address distinct problems entirely, such as the design and sizing of energy systems [19], vehicle to grid (V2G) [20], or focus on grid functionality and operational issues, using power system analysis such as stability, power quality, and power flow [21,22]. To provide a structured overview, the following subsections categorize the main coordination schemes found in the literature. Specifically, different control approaches for coordinating agents (EV chargers, HEMS, or other applications) can be broadly classified into direct and indirect coordination frameworks [1].

1.2.1. Indirect coordination

In an indirect coordination scheme, agents indirectly coordinate through Demand Response (DR) price signals without exchanging messages and team objectives using a decentralized decision-making framework.

Indirect HEMSs coordination. Numerous works have highlighted the matters of indirect coordination of agents in HEMS [11,23–28] applications. [23] devised an energy sharing management framework by a Stackelberg game to orchestrate collaborative energy sharing among prosumers, thereby maximizing the utilities of both prosumers and the grid operator through indirect coordination strategies. [24] proposed a distributed energy management system based on the Stackelberg game, elucidating the Pareto front regarding trade-offs between consumer welfare and retailer profit, with consumer behavior influenced indirectly through day-ahead pricing strategies. Adika et al. [25] developed dynamic pricing using a non-cooperative Nash equilibrium game, indirectly coordinating storage batteries in homogeneous consumer grids based on power surplus/deficit profiles. [27] proposed a decentralized multi-agent HEMS system where agents adjust decisions based on dynamic prices without direct communication or shared objectives, thereby achieving individual goals indirectly. Safdarian et al. [26] explored decentralized and indirect coordination of HEMSs to mitigate rebound peaks, facilitated by transmitting desired profiles. [11] introduced a distributed demand response program using proximal decomposition to indirectly coordinate thermal storage systems in a residential cluster, utilizing dynamic pricing to reduce overall consumption

Indirect EVs coordination. Several studies have explored the indirect EVs charging coordination as reflected in works by [29–32]. [29] devised a stochastic dynamic programming framework for optimizing energy management in smart homes with plug-in EVs (PEV) energy storage, aiming to minimize electricity costs while meeting power demand and charging needs, evaluated under time-varying electricity prices and weekdays power demands. [30] developed a game-theoretic approach to distributed charging control for plug-in EVs in distribution networks, ensuring cost minimization for individual customers while meeting network security constraints. [31] introduced a transaction and centralized real-time EV charging management scheme for commercial buildings with PV generation and EV charging services, optimizing charging under uncertainties while respecting EV owners' preferences and achieving cost-effective demand response coordination. [32] presented a centralized non-cooperative approach for orchestrating EVs and household appliances, with the utility indirectly coordinating through sharing aggregated demand updates.

1.2.2. Direct coordination

Conversely to indirect coordination, direct coordination can occur through message exchanges between end-user agents or via an intermediary using a third-party entity such as a coordinator, with various topologies facilitating this process [1,2].

1.2.2.1. Direct HEMSs coordination. Multiple studies have explored direct coordination between HEMSs. [1] elaborated a distributed coordination technique for HEMSs with demand response-enabled electric heaters, aiming to mitigate the negative impacts of uncoordinated HEMSs on the distribution system. The proposed technique achieves consensus among HEMSs to optimize individual and shared objectives, as evidenced by simulation results showcasing enhanced peak shaving and reduced electricity bills. Souza et al. [33] proposed a bi-level optimization for coordination of HEMSs, optimizing energy costs and user comfort at the first level and minimizing total electricity costs and incentives at the aggregator level using distributed Dantzig–Wolfe decomposition. [34] designed a novel control that orchestrates air conditioning load clusters. In this framework, each HEMS optimizes its AC loads in response to a dynamic regulation signal from the coordinator, who continually adjusts this signal based on user inputs to achieve the desired target. Zhang et al. [35] studied demand response using a bi-level game model, initially using indirect coordination through price adjustments and later transitioning to direct coordination with information sharing among consumers. [36] developed a centralized coordination approach using Shapley game theory to minimize collective energy costs but faced challenges due to computational complexity and the absence of a gain-sharing mechanism among players. [37] explored decentralized and centralized methods for coordinated load management but lacked an incentive policy and mechanism to distribute penalties based on consumers' contributions. In a distribution system characterized by highly distributed generation, end-users form coalitions to maximize their payoffs and profits using a game theory-based HEMS, as presented by Zhang et al. [7].

1.2.3. Direct EVs coordination

[38] developed a distributed coordination strategy through a Nash bargaining game-theory-based peer-to-peer transactions to maximize charging stations' profits. Analytical target cascading (ATC) and alternating direction method of multipliers (ADMM) have been used to solve the direct coordination problem with a bi-level parallel coupling framework. In [39], the problem is transformed into a distributed scenario by employing decomposition techniques for joint optimization of optimal power flow (OPF) and EV charging, solved iteratively in a nested manner. [40] implemented a primal–dual subgradient method for EV control within a residential distribution network. These studies offered a robust EV charging algorithm; however, they overlook addressing uncertainties in EV charging schedules and fulfilling network-level constraints such as voltage fluctuations induced by EV control in the distribution grid. [41] presented a multiagent system for EV charging control. The authors investigated the bidding strategy for EV energy injection into the grid and proposed energy management strategies based on it. Oshnoei et al. [42] implemented a two-layer model predictive control to improve the response of battery energy storage systems for primary frequency control. The authors in [43] proposed a multiagent-based control structure for EV charging, considering factors like driver behavior, charging station location, and electricity price. However, their focus remained on EVs and charging strategy without addressing the impact of their algorithm on the distribution grid. The research detailed in [44] introduced a chance-constrained energy management system using the ADMM to handle the stochastic nature of EVs and addressed an EV charging scheduling optimization problem. While it effectively addressed EV randomness, the study did not thoroughly examine the impact of the proposed charging solution on the distribution grid. Fan et al. [45] developed a distributed ADMM-based multi-period problem, wherein the DSO addressed OPF issues with a substantial influx of controlled EVs managed by aggregators. Their approach also emphasized the maintenance of critical grid security parameters, including voltage limits and transmission line capacities. A similar EV charging and grid voltage stability objective is discussed in [46]. The authors addressed a complex objective function with interconnected power flow constraints using a decentralized hierarchical ADMM-based

method. The ADMM-based methods discussed above utilized iterative techniques in discrete time, highlighting the significance of sampling frequency for result accuracy. Given the intermittent nature of EV charging, a minimal sampling interval is crucial for real-time optimization dynamics, ensuring the sustained optimality of solutions over time steps. The work in [47] presented a real-time EV charge scheduling solution using a dynamic non-cooperative game method, employing ADMM for problem decomposition and real-time solution implementation. While the results are intriguing for real-time applications, the study overlooks the effects of charging scheduling on distribution grid metrics like voltage. [48] introduced a distributed real-time ADMM technique for controlling EVs and BSSs, addressing voltage regulation while maximizing utility. However, scalability challenges in real-world implementation were not thoroughly explored, and communication overhead in distributed control was not extensively analyzed. Further investigation is warranted to assess system robustness under varying conditions.

1.3. Literature limitations summary

The literature limitations identified in prior research include:

- Lacks of exploration of establishing a global consensus among HEMSs and CSMS, sharing team objectives, and complementary actions through a distributed framework. This gap is particularly significant for addressing local grid challenges arising from high EV penetration and winter peak loads.
- Exploring a method to accurately gauge HEMS and CSMS agents contributions in coordination, and fairly gain allocation of collective gains among agents, remains unexplored.
- Insufficient focus on incentive mechanisms that encourage voluntary participation without penalizing users.

To the authors' knowledge, no prior works in the literature address all these aspects collectively.

1.4. Main contributions

This study targets the outlined limitations and seeks to bridge existing gaps in research. The primary contributions of this investigation are outlined as follows:

- **Integrated Distributed Coordination with Privacy-Preserving Consensus:** We develop a modular, agent-based framework where HEMS and CSMS agents coordinate through a non-punitive consensus and sharing mechanism. This distributed approach facilitates the sharing of collective objectives among agents to enable them to reach a global agreement, such as meeting grid constraints, enhancing load factor, and reducing energy bills—and facilitates synchronized, complementary actions. The coordination is inherently privacy-preserving, as it relies on aggregated energy profiles rather than sensitive individual data, distinguishing it from centralized alternatives. The framework is designed to balance individual goals with collective needs, preserve user autonomy, and achieve Pareto efficiency, guaranteeing that no agent is disadvantaged by participating.
- **Contribution-Based Non-Punitive Incentive Allocation:** We introduce a novel non-punitive incentive and gain-sharing mechanism grounded in Shapley value theory, enabling fair and transparent distribution of coordination gains according to each agent's quantified marginal contribution without imposing monetary pen alties for consumers. This approach transparently rewards agents based on their flexibility, promoting equitable reward allocation.
- **Benchmark for Future Research:** This work provides a transparent benchmark for evaluating residential coordination frameworks, focusing on the core effects and benefits of coordination, and enabling meaningful assessment.

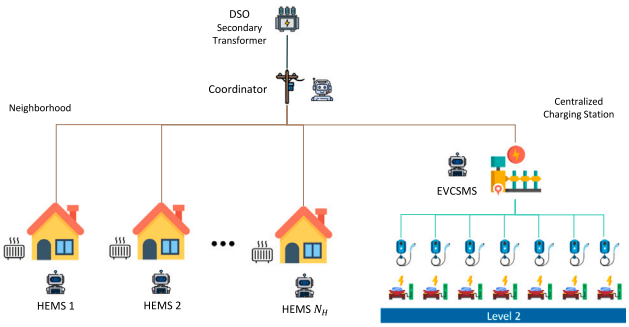

Fig. 1. The coordination framework of HEMSs and CSMS in a residential neighborhood.

The rest of this paper is structured as follows. Section 2 designs the CSMS and HEMSs coordination system framework. Section 3 introduces the neighborhood system model, including residential consumers and EV charging station sub-models. Section 4 elaborates on the proposed optimization problem formulations to implement the coordination between CSMS and HEMS. Section 5 defines the Case studies and analyzes the effectiveness of the proposed coordination method for HEMSs and CSMS, presenting the numerical results concisely. Finally, Section 6 briefly summarizes the paper's findings and conclusions.

2. Coordination system framework

Let us delve into the system framework, consisting of N_H houses equipped with HEMSs controlling flexible loads, an electric vehicle Charging Station (CS) managed by a CSMS handling N_{EV} EVs, alongside a neighborhood coordinator and the distributed system operator (DSO) representative, illustrated in Fig. 1. The network illustrated in Fig. 1 represents a typical residential setting, where EV charging is supported by Level 2 chargers [49,50]. These chargers operate on a standard 240 V single-phase circuit, consistent with the electrical supply commonly available in residential areas.

The decision-making mechanism in the system is orchestrated among four types of agents: HEMSs agents, the CSMS agent, the neighborhood coordinator agent, and the DSO agent. A single distribution transformer serves the EV Charging Station and all houses. The Distribution System Operator provides the necessary energy supply and broadcasts the electricity rates. The DSO plays a crucial role in implementing a mechanism to incentivize both CS (and thus EV owners) and residential consumers to engage in the coordinated demand response program actively. One emerging mechanism for this purpose is reward policies, which may involve monetary incentives or energy credits based on the level of flexibility users provide to support ancillary services. Individual customers' and CS' rewards can be contingent upon their level of participation in the global coordination and their contributions to the overall coordination scheme. These rewards are distributed among them by the coordinator based on their marginal contributions. Each residence includes both non-flexible and flexible loads, with the latter serving as the source of user flexibility in demand response programs. The HEMS in each house regulates electric heaters (EHs) based on the user's flexibility level, which includes indoor temperature set-points and comfort preferences in demand response programs. The CS implements a charging strategy for all EVs to minimize operational costs and meet user preferences. The CSMS functions as an independent decision-maker, ensuring EV owners' energy needs are met and reducing charging costs through coordination program participation. It retains full autonomy, choosing whether to participate and determining charging amounts, such as bypassing coordination to charge immediately upon connection, with costs calculated based on a DSO-generated price signal disseminated by the coordinator agent. The neighborhood coordinator's role

involves orchestrating demand responses between CSMS and HEMSs to reach a consensus that aligns with the collective goals of the team while also considering each agent's individual objectives and constraints. Acting as a consumer representative, the coordinator seeks to enhance the team's total gain by coordinating efforts to meet the DSO's objectives and address specific challenges within the local grid. The coordinator is tasked with safeguarding user privacy, ensuring reliable and secure data communication among agents, measuring agents' contributions to the coordination, and subsequently distributing total gained rewards accordingly. Therefore, the coordinator must dynamically manage HEMSs and CS charging schedules to ensure that the overall increase in grid power demand remains within acceptable limits, thereby lowering operating costs for the DSO. This involves coordinating flexible load handling by HEMSs and EV charging program management by CSMS through a streamlined message exchange framework, while also safeguarding user privacy. By orchestrating the charging of the EV fleet and residential flexible loads, the coordinator negotiates advantageous incentives and energy tariffs with the DSO, leveraging solving grid challenges and cost reduction as bargaining chips. The proposed distributed coordination framework is designed for high versatility, capable of adapting to neighborhoods with diverse types of flexible loads beyond electric baseboard heaters, such as heat pumps, water heaters, smart appliances, or even distributed generation and storage. The fundamental coordination framework remains same and robust, as its core principle involves accurately modeling the operational characteristics of each flexible asset and integrating these models into the local optimization problem of the HEMS or CSMS. This allows the framework to leverage any provided flexibility, irrespective of its source. For instance, extending the HEMS to incorporate heat pumps or various smart appliances simply requires including their specific mathematical models and constraints. This inherent adaptability ensures the coordination mechanism remains effective and efficient across varied setups without changing the coordination procedure, even when consumers possess different combinations of flexible assets.

3. System model

As depicted in Fig. 1, the neighborhood comprises $\mathcal{N}_{\mathcal{H}}$ houses with HEMSs, one charging station (CS) managed by a CSMS handling $\mathcal{N}_{\mathrm{EV}}$ EVs, a coordinator, and the DSO. At the coordinator level, the residential neighborhood is supplied by a common distribution transformer and interconnected through shared connections. The tie-connections at the DSO and coordinator levels are subject to capacity constraints, as specified by,

$$\left|\sum_{i=1}^{N_N} E_{i,max}^{\mathrm{NT}}\right| \leqslant E_{\max}^{\mathrm{DT}}, \quad \& \quad \left|\sum_{i=1}^{N_H} E_i^H + E^{\mathrm{CS}}\right| \leqslant E_{\max}^{\mathrm{NT}}. \tag{1}$$

Where $E^{\mathrm{CS}} = \sum_{v=1}^{N_{\mathrm{EV}}} E_v^{EV}$ The energy consumption constraints for the CS and houses are also specified by,

$$E_{min}^{\mathrm{CS}} \leqslant E^{\mathrm{CS}}(h) \leqslant E_{\max}^{\mathrm{CS}} \quad \& \quad E_{min}^{H} \leqslant E^{H}(h) \leqslant E_{\max}^{H} \tag{2}$$

Let $\mathcal{H} = 1, 2, \ldots, h$ indicate the time horizon set, with measurements taken every 15 minutes throughout the day, resulting in $h = 96$ intervals. This division means the interval $[1, h]$ is segmented into h 15-minute intervals. Both HEMSs and CSMS agents have the ability to adjust and schedule their flexible loads.

While this work integrates seasonal variations in EV charging efficiency (based on temperature) and models residential consumer preferences and EV chargers using real data and machine learning (normal distributions), we acknowledge other real-world uncertainties. However, to clearly highlight the core benefits of our proposed coordination framework as a benchmark, we deliberately did not explicitly model uncertainties with potentially larger impacts, such as unexpected changes in user preferences, occupancy patterns, or EV charging behaviors. It is noteworthy that the distributed and iterative nature of our algorithm provides inherent adaptability, allowing agents to re-optimize and adjust to dynamic conditions during the negotiation process. This work serves as a foundation for future research to explicitly address these broader uncertainties, including those related to system models, communication failures, and distributed energy generation fluctuations.

3.1. House model

Each household's HEMS manages electric heaters as flexible loads for participation in the coordinated demand response program and consumer comfort satisfaction, while fixed loads operate based on standard energy consumption patterns and are not flexible during coordination. The indoor temperature (T_i^{in}) of each household is a state variable demonstrated as $T_i^{\mathrm{in}} = \left[T_i^{\mathrm{in}}(1), T_i^{\mathrm{in}}(2), \ldots, T_i^{\mathrm{in}}(h)\right]$. The relation among electric heater's energy consumption profile (E_i^{EH}), indoor temperature (T_i^{in}), and outdoor temperature (T^{in}) is modeled using a linear thermal model [51], and the house thermal dynamic response is modeled through the state-space representation denoted by Eq. (3), where α_i (state matrix), β_i (input matrices associated with the heater), and γ_i (input matrices associated with the weather) are thermal coefficient parameters. These parameters are estimated using experimental data and applying a ridge regression approach [52,53] for system identification.

$$T_i^{\mathrm{in}}(h+1) = \alpha_i T_i^{\mathrm{in}}(h) + \beta_i E_i^{\mathrm{EH}}(h) + \gamma_i T^{\mathrm{out}}(h) \tag{3}$$

The fixed loads are modeled based on recorded data from experiments, including all user energy consumption except electric heater consumption. Eq. (4) represents the total energy demand of each household, where E_i^{FL} denotes the total loads' consumption except the heater.

$$E_i^H = E_i^{\mathrm{EH}} + E_i^{\mathrm{FL}} \tag{4}$$

The energy cost of each house is computed by,

$$C_i = \sum_{h=1}^{h} \theta(h) E_i^H(h) \tag{5}$$

A quadratic utility function in (6) models the discomfort, where ω_i defines comfort levels and can take values from the set $\Omega \in [\omega_{\min}, \omega_{\max}]$, which $\omega_{\min} = 0$. Additionally, the parameter $\omega_{\max}$ in (6) was derived from a log-normal distribution with variance $Var(\omega_{\max}) = 1$ and expectation $\mathbb{E}(\omega_{\max}) = 5$, shaping the setpoint profiles and house preferences based on these distributions.

$$D_i = \omega_i(h)\left(T_i^{\mathrm{SP}}(h) - T_i(h)\right)^2 \tag{6}$$

Constraints on indoor temperature and heater energy consumption are represented by (7). Consumer preferences in indoor temperature set-points and comfort zones are modeled based on experimental data and ASHRAE Standard-55-2004.

$$T_i^{\mathrm{in}} \in [T_{i,\min}^{\mathrm{in}}, T_{i,\max}^{\mathrm{in}}] \quad \& \quad E_i^{\mathrm{EH}} \in [E_{i,\min}^{\mathrm{EH}}, E_{i,\max}^{\mathrm{EH}}] \tag{7}$$

The comfort preferences and power consumption profiles of houses in Trois-Rivières, Québec, were modeled using statistical data excluding electric heaters. A semi-synthetic data-driven model was developed using this data to simulate non-flexible load profiles, combining both flexible (heaters) and non-flexible loads to create an aggregated consumption profile. The consumers' set-point temperature T_i^{SP} was devised from the experimental data, with thermostats stochastically programmed based on the distribution of set-point temperature T_i^{SP}, which ranges from 20 to 23 degrees Celsius with probabilities $P(T_i^{SP}) = [0.1, 0.3, 0.5, 0.1]$. The minimum indoor temperatures $T_{i,\min}^{\mathrm{in}}$ were calculated as $T_{i,\min}^{\mathrm{in}} = T_i^{SP} - T_i^{\delta}$, where T_i^{δ} is a discrete random variable with values $1, 2, 3, 4$ in Celsius and probabilities $P(T_i^{\delta}) = [0.1, 0.3, 0.4, 0.2]$.

The HEMS model is designed to manage diverse flexible loads or assets within individual homes. While this paper primarily focuses on electric baseboard heaters as the flexible load, the framework is

capable of seamlessly integrating other new flexible assets and loads, such as PV, heat pumps, electric water heater, smart appliances, or individual EV chargers. This adaptability allows for different homes to participate with varying types and combinations of flexibility sources, as the coordination process is asset-agnostic and relies on the HEMS to accurately model and optimize its specific controllable devices without requiring changes to the core coordination framework.

3.2. Charging station model

The individual EV charging is managed by the CSMS (Charging Station Management System) based on the arrival battery SOC, desired SOC and parking duration. The SOC of each EV index v ($v \in \mathcal{V}$) is modeled using the Coulomb counting technique described by:

$$\mathrm{SOC}^v_{h+1} = \mathrm{SOC}^v_h + \hat{\eta}^v_{c,T} \frac{p^v_h \Delta t}{Q^v_{\mathrm{cap}}} s^v_h u^v_h, \quad v \in \mathcal{V} \tag{8}$$

where SOC^v_h indicates the state of charge of the battery at the time step h. s^v_h and u^v_h are binary variables used by the CSMS to manage the charging process. s^v_h denotes the parking status of the EV, being 1 when the EV is parked (from plug-in to plug-out) and 0 otherwise. Similarly, u^v_h is a control signal that turns the EVSE (Electric Vehicle Supply Equipment) charging ON or OFF. $\hat{\eta}^v_{c,T}$ and Q^v_{cap} represent the charging efficiency in % and battery capacity in kWh, respectively. The variable p^v_h denotes the charging power (in kW), and Δt corresponds to the time step duration (15 min, or 0.25 h). When considering vehicle-to-grid (V2G) operations, the charging power p^v_h can take negative values to represent discharging from the EV to the grid. In this case, the charging efficiency $\hat{\eta}^v_{c,T}$ should be replaced with the discharging efficiency $\hat{\eta}^v_{d,T}$, which is typically slightly lower than the charging efficiency due to additional conversion losses [20]. It is important to note that frequent V2G operations may accelerate battery degradation, and a trade-off should be considered in practical implementations.

Most EVs utilize the Constant Current-Constant Voltage (CCCV [54–56]) charging mode, leading to non-linear behavior in charging power and a linear time-variant state equation, as shown in (8) [57]. This can be approximated using an average charging power profile. Given the battery capacity, initial SOC, and charging efficiency, the state dynamics can be expressed in terms of the energy state as:

$$x^v_{h+1} = x^v_h + \hat{\eta}^v_{c,T} \frac{\hat{P}^v_{\mathrm{av}} \Delta t}{Q^v_{\mathrm{cap}}} s^v_h u^v_h, \quad v \in \mathcal{V} \tag{9}$$

Where x^v_h represents the accumulated energy in kWh charged to EV v since it was plugged in, and $\hat{P}^v_{\mathrm{av}}$ is the estimated average charging power. The state constraints are defined as :

$$x^v_{t^v_a} = 0 \tag{10}$$

$$x^v_{t^v_d} \geq \hat{x}^v_{\min} \tag{11}$$

$$s^v_h = \begin{cases} 1 & \text{if } t^v_a \leq h \leq t^v_d \\ 0 & \text{else} \end{cases} \tag{12}$$

where $\hat{x}^v_{\min} = Q^v_{\mathrm{cap}} \left(\mathrm{SOC}^v_{\mathrm{desired}} - \mathrm{SOC}^v_{\mathrm{initial}}\right)$ defines the minimum energy that needs to be charged to the EV to satisfy the user's preferred state of charge $\mathrm{SOC}^v_{\mathrm{desired}}$. t^v_a and t^v_d indicate the EV's arrival and departure times, respectively.

The average charging power $\hat{P}^v_{\mathrm{av}}$ is estimated based on the initial and desired SOC, battery capacity, and historical charging profiles. It can be approximated using the reference power in the constant current phase, P_{CC}, typically 3.3 kW for Level 1 charging (120V) and 6.6 kW/7.3 kW for Level 2 charging (240V) if the desired SOC at the expected departure time is less than 80%. The CSMS can control this rate via the control pilot for the SAE J1772 charging standard. The same protocol can be used by the CSMS to detect EV plug-in and plug-out time, hence s^v_h. However, when the desired SOC at departure exceeds 80%, the average power can be estimated using historical charging profiles from complete sessions. The energy requirement for the constant voltage (CV) phase is derived from these profiles [58], while the constant current (CC) phase requirement is calculated as:

$$\hat{x}^{CC,v}_s = \hat{x}^v_{\min} - x^{CV,v}_l \tag{13}$$

where in the current session, s, $x^{CC,v}_s$, and $x^{CV,v}_l$ are the energy demand in the CC and CV phases, respectively.

The duration of the CC phase, in terms of the number of simulation time steps h, $\hat{t}^{CC,v}_s$, is estimated by:

$$\hat{t}^{CC,v}_s = \frac{\hat{x}^{CC,v}_s}{\hat{P}^v_{\mathrm{av}}} \frac{60}{\Delta t} \tag{14}$$

The charging profile is then constructed as follows:

$$\hat{P}^v_h = \begin{cases} P^v_{\mathrm{CC}} & \text{for } h \in \left[t^v_a, \hat{t}^{\mathrm{CC},v}_s\right] \\ P^{\mathrm{CV},v}_{h,s*} & \text{for } h \in \left[\hat{t}^{\mathrm{CC},v}_s : \hat{t}^{\mathrm{CC},v}_s + t^{\mathrm{CV},v}_l\right] \end{cases} \tag{15}$$

Where $P^{\mathrm{CV},v}_{h,s*}$ is the charging power during the CV phase, recorded from the last (most recent) full charge for the same charging condition. The average of this constructed power profile provides $\hat{P}^v_{\mathrm{av}}$ for the state equation.

The temperature effect is a critical aspect of EV charging, particularly in winter and cold regions. Low temperatures increase the battery's internal resistance, slowing down electrochemical reactions and extending charging duration. To account for the temperature effect, EV charging efficiency loss is modeled by a third-order polynomial:

$$\hat{\eta}^v_{c,T} = aT^3 + bT^2 + cT + d \tag{16}$$

This model captures the non-linear relationship between temperature and charging efficiency loss, enabling the CSMS to predict battery behavior over a range of temperatures. This directly impacts charging duration and scheduling to meet user preferences. Parameters a, b, c, and d can be determined through experimental data fitting under controlled temperature environment tests or using machine learning techniques with historical charging session records. Fig. 2 illustrates the variation of a typical Lithium battery capacity with respect to the temperature [59]. Fig. 3 presents an EV charging session based on the CCCV modes, highlighting the uncertainty in the charging profile due to external factors such as ambient temperature.

This profile is similar to the one observed in DC fast charging, with the key difference being the addition of a conditioning phase prior to the high-current regulation phase in the constant current (CC) stage to ensure battery safety. It is also strongly recommended to stop charging (unplug) at the end of the CC phase, typically when the battery reaches around 80% state of charge (SOC) for DC fast charging.

The total energy demand of the charging station E^{CS} and the energy cost C_{CS} of the charging station is determined by,

$$E^{\mathrm{CS}} = \sum_{h=0}^{H-1} \left(\sum_{v=1}^{N_{\mathrm{EV}}} E^v_h \right) \tag{17}$$

$$C_{\mathrm{CS}} = \sum_{h=0}^{H-1} \theta_h \left(\sum_{v=1}^{N_{\mathrm{EV}}} E^v_h \right) \tag{18}$$

Where $E^v_h = \hat{P}^v_{\mathrm{av}} \Delta t s^v_h u^v_h$ is the energy charged to EV v at each time step h.

3.3. EVs charging model for the CSMS agent

The charging stations, as part of the neighborhood, are managed by a centralized controller CSMS. The main goal of this CSMS is to coordinate EV charging with respect to the overall aggregate demand of the neighborhoods. By participating in this overall aggregate demand management, the CSMS ensures a reduction in the charging cost for

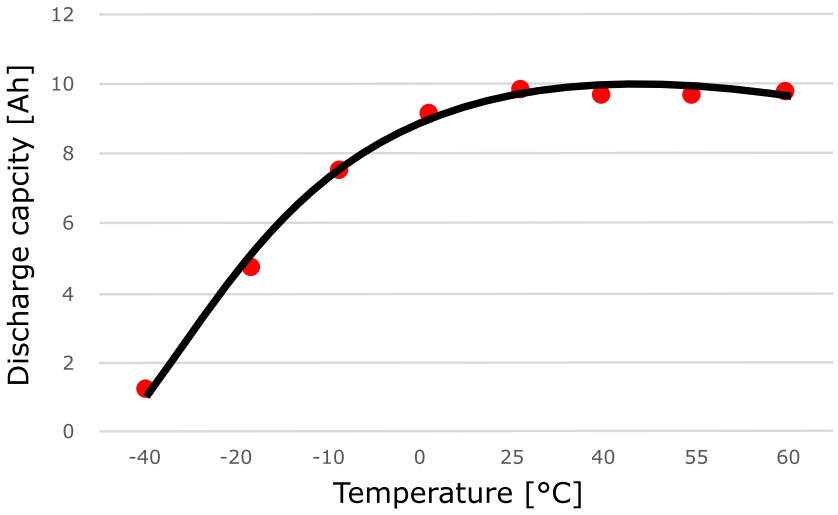

Fig. 2. Discharge capacity of a typical lithium cobalt oxide battery with a rating of 10 Ah at different temperatures [59].

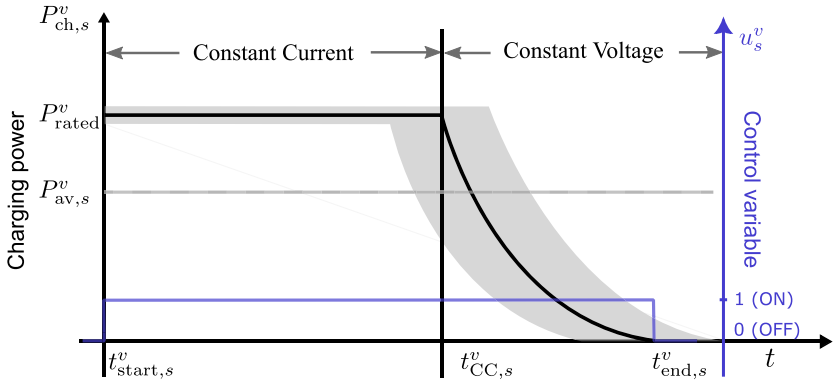

Fig. 3. Typical EV charging process with a fixed charging rate at AC level 1 and 2 EVSE charger.

individual EVs while meeting their charging need in terms of the energy requirements for their future trips.

Let H be the optimization horizon, $\hat{P}^v_{\text{av}}$ the average charging power for each EV $v \in \mathcal{V}$ and the θ an array representing the electricity price over the horizon H. The CSMS in the first iteration solves the following mathematical optimization problem to define the optimally controlled input $u^{v,*}_h$ for each EV at each time index h with respect to the individual desired $x^v_{\min}$ and the estimated departure/plug-out time.

$$\underset{\{u^v_h, x^v_h\}^{v\in\mathcal{V}}_{h\in\mathcal{T}}}{\arg\min} \quad J^{\text{CS}} = \sum_{h=0}^{H-1}\left(\sum_{v=1}^{N_{\text{EV}}} \theta_h \hat{P}^v_{\text{av}} \Delta t\, s^v_h u^v_h\right) \tag{19a}$$

$$\text{subject to} \quad (9)\text{–}(11), \tag{19b}$$

$$0 \le u^v_h \le 1, \qquad v \in \mathcal{V}, h \in \mathcal{H} \tag{19c}$$

After the CSMS solves the selfish optimization (uncoordinated case) in (19a)–(19c) with respect to other loads in the neighborhood, the coordination phase is engaged in the following iterations and the CSMS updates its decisions to participate in the coordination. In the coordination case, during the iterative negotiation process with the coordinator, the CSMS sends the aggregated scheduled energy demand $\sum_{v\in\mathcal{V},h\in\mathcal{H}} u^{v,*}_h P^v_{\text{av}} \Delta t$ obtained by solving (19a)–(19c) to the neighborhood energy demand coordinator. At this step, the coordinator calculates the global and dual optimization variables to coordinate EV charging with respect to the other home energy management systems in the neighborhood and sends the updated global/dual variables back to the CSMS. This process will be continued until all agents in the neighborhood reach a global agreement. The details and the coordination problem will be presented in the next section.

Note that the decision to charge each EV v, represented by the binary variable u^v_h, is taken by a centralized CSMS. This holds true whether the EVSEs are physically connected to the same electrical panel fed by a dedicated transformer (as shown in Fig. 1) or if each neighborhood house EVSE communicates critical parameters (such as t^v_a, t^v_d, and E_{ch}) to the CSMS. This underscores the transversality of the proposed coordination framework.

Notably, the actual charging cost for fast chargers (Level 3) is typically higher than that of slower chargers (Level 2) due to the high infrastructure costs [49]. Consequently, car owners generally use fast chargers for emergency charging only. Level 3 chargers, also known as DC Fast Chargers, provide significantly faster charging. However, these chargers require higher-voltage three-phase power, which is uncommon in residential settings, and their installation is often cost-prohibitive due to the need for substantial upgrades to the MV/LV transformer and local grid infrastructure [54]. Furthermore, frequent use of Level 3 charging can accelerate battery degradation, making it less suitable for daily residential use [60]. In contrast, Level 2 chargers align with the single-phase 120/240V supply common in residences, providing practical charging speeds suitable for overnight charging and compatible with typical residential energy consumption patterns [49]. Given their practicality and alignment with residential infrastructure, this study focuses primarily on Level 2 chargers as the standard for residential applications. While a comparative analysis of Level 2 and Level 3 chargers is included to highlight their differences, all analyses

in this paper are based on the use of Level 2 chargers due to their predominant role in residential settings.

4. Proposed CSMS and HEMSs coordination

This section introduces a centralized coordination technique aimed at establishing consensus and distributing shared objectives among CSMS and HEMSs. Following this, a distributed coordination technique is developed. Lastly, a reward-sharing mechanism is proposed.

4.1. Proposed centralized CSMS and HEMSs coordination

Our proposed CSMS and HEMSs coordination approach is outlined in this subsection. The coordination aims to fulfill individual and collective objectives, addressing local grid challenges. The team objective J^{joint} is a function of the sum of CSMS and HEMSs energy profiles. The coordination problem is formulated centrally as,

$$\begin{aligned}\min_{E_i^H, E^{\text{CS}}} \ & \sum_{i=1}^{N_H} J_i^H\left(E_i^H\right) + J^{\text{CS}}\left(E^{\text{CS}}\right) \\ & +\text{CR}\ J^{\text{joint}}\Big(\sum_{i=1}^{N_H} E_i^H + E^{\text{CS}}\Big), \\ & \textit{subject to}: (1)-(11), (19c)\end{aligned} \tag{20}$$

The coordination problem aims to find an equilibrium that balances joint objectives with individual goals. It employs a convex optimization approach, ensuring that every local minimum is also a global minimum within convex sets. At the equilibrium point, all participants achieve optimal decisions, meeting both individual and joint objectives. Adjusting the coordination level parameter CR allows for control over the emphasis placed on joint versus individual goals. The individual objective function for each HEMS is defined by,

$$J_i^H = C_i + D_i \tag{21}$$

4.2. Proposed distributed CSMS and HEMSs coordination

While effective in mitigating issues from uncoordinated HEMSs, the centralized coordination method requires significant computational resources and processing time. Thus, this subsection introduces the coordination methodology, detailing agent interactions for distributed coordination. The distributed coordination approach streamlines computations across multiple processors, leading to reduced processing time. The proposed distributed coordination approach involves several key players: HEMSs, CSMS, coordinator, and DSO. Initially, the coordinator gets electricity rates and incentive policies from the DSO to handle local grid challenges and gathers baseline profiles (no demand response case) from each household. Using this data, the coordinator computes the initial aggregated profile and updates global and dual variables to guide HEMSs and CSMS towards achieving both individual and collective goals. Then, HEMSs and CSMS agents receive input on electricity price and updated global and dual variables from the coordinator. Subsequently, each agent engages in convex optimization to minimize electricity costs, enhance comfort, and maximize their share of the team's total gain by contributing effectively to the coordination. After optimization, each consumer computes the optimal load profile and transmits it to the coordinator. On the coordinator's side, convex optimization is also conducted to fulfill several primary tasks, including smoothing the aggregated profile to improve load factor, reducing the aggregate electricity bill for the team, maximizing total team incentives, ensuring fair distribution of rewards among HEMSs and CSMS, facilitating data exchange among participants, and negotiating with the DSO regarding reward rates and desired load factors. This iterative negotiation process between the coordinator and team members (HEMSs and CSMS) will continue until the coordinator exhausts all team flexibility, reaches a consensus, and is unable to update global or dual variables anymore. The collaborative efforts of HEMSs and CSMS result in accomplishing shared objectives and attaining overall gain. Each agent receives a share of the gain proportionate to its marginal contribution compared to other members. The coordination is structured as a mutually beneficial arrangement, promoting collective benefits. The following section elaborates on the proposed distributed coordination procedure, employing the Alternating Direction Method of Multipliers (ADMM). The distributed coordination between N agents including N_H HEMSs and one CSMS is elucidated by,

$$\begin{aligned}\underset{E_i^H \& E^{\text{CS}} \& \bar{Z}}{\text{minimize}} \ & \sum_{i=1}^{N_H} J_i^H\left(E_i^H(h)\right) + J^{\text{CS}}\left(E^{\text{CS}}(h)\right) \\ & +\text{CR}\ J^{\text{joint}}\left(N\bar{Z}(h)\right), \\ s.t.: \ & \bar{Z} = \left(\frac{1}{N}\right)\sum_{j=1}^{N} Z_j \ \&\ E_j - Z_j = 0, \\ & (1)\text{–}(19c) \ \setminus \{(19a)\}.\end{aligned} \tag{22}$$

The problem represented byEq. (22) is transformed into a distributed problem focusing on sharing and consensus. This transformation is achieved through the scaled form of ADMM, as shown in Eqs. (23) through (25).

$$\begin{aligned}E_i^{H,k+1} := \ & \underset{E_i^H, i\in[1,N_H]}{\text{argmin}} \ J_i^H\left(E_i^H\right) \\ & + \frac{\rho}{2}\left\|E_i^H - E_i^{H,k} + \bar{E}^k - \bar{Z}^k + \lambda^k\right\|_2^2\end{aligned} \tag{23}$$

$$\begin{aligned}E^{\text{CS},k+1} := \ & \underset{E^{\text{CS}}}{\text{argmin}} \ J^{\text{CS}}\left(E^{\text{CS}}\right) \\ & + \frac{\rho}{2}\left\|E^{\text{CS}} - E^{\text{CS},k} + \bar{E}^k - \bar{Z}^k + \lambda^k\right\|_2^2\end{aligned} \tag{24}$$

$$\begin{aligned}\bar{Z}^{k+1} := \ & \underset{\bar{Z}^k}{\text{argmin}} \ \text{CR}\ J^{\text{joint}}\left(N\bar{Z}^k\right) \\ & + \frac{N\rho}{2}\left\|\bar{Z}^k - \lambda^k - \bar{E}^{k+1}\right\|_2^2\Big)\end{aligned} \tag{25}$$

$$\lambda^{k+1} = \lambda^k + \bar{E}^{k+1} - \bar{Z}^{k+1} \tag{26}$$

where $\bar{E} = \frac{\left(\sum_{i=1}^{N_H} E_i^H\right) + E^{\text{CS}}}{N}$ is the average of all HEMSs and CSMS agents. The coordination procedure involves several steps, with each agent carrying out specific tasks independently in a parallel manner. HEMS agents execute the E^H-update step (given by (23)) in parallel, while the CSMS agent performs the E^{CS}-update step (given by (24)). The coordinator then aggregates the decisions from all agents to form the average $\bar{Z}$ in the $\bar{Z}$-update step (25), which is crucial for satisfying joint objectives. Additionally, the λ-update step (indicated by (26)) involves updating the dual variable, allowing the coordinator to adjust global and dual variables and transmit them to all agents for consensus building. This iterative process continues until either the dual-residual is close to zero or the maximum iteration count is reached, ensuring convergence towards joint objectives. The team's shared objectives prioritize flattening the aggregated consumption profile and minimizing overall energy costs, ensuring optimal outcomes for both individual and joint goals.

$$J^{\text{joint}}\left(N\bar{Z}\right) = \left\|N\bar{Z} - \left(\sum_{h=0}^{H}\frac{N\bar{Z}_h}{H}\right)\right\|_2^2 + \left\|\sum_{h=0}^{H} N\bar{Z}_h\right\|_2^2, \tag{27}$$

The coordination level CR signifies the degree of emphasis placed on joint objectives relative to individual goals, with CR being selectable from the range $CR \in [0, 1]$. A CR value of 0 indicates no coordination among agents, while CR of 1 signifies maximal coordination for shared goal attainment. In a real-world setting, the value of CR would be determined through negotiation between the coordinator and the DSO, driven by the DSO's specific challenges (e.g., improving load factor) and the total negotiated reward for collective benefits. Agents delegate their

decision-making about team's coordination level to the coordinator, trusting it to represent their interests in these negotiations. The CR parameter and joint objectives can be updated post-negotiation, where the DSO aims to resolve local grid challenges through joint objectives, while the coordinator seeks to enhance the team's gains by negotiating reward rates. The optimal CR value is sensitive to the team's aggregate flexibility and the negotiated reward rate; for instance, if no flexibility remains, increasing CR will have no further effect, or a low reward rate might lead to a lower chosen CR. For the case studies in this paper, the CR is assumed to be pre-defined based on such negotiation.

The algorithm 1 delineates and summarizes the step-by-step process of implementing the coordinated CSMS and HEMSs, focusing on achieving consensus and sharing joint objectives.

Algorithm 1: Coordination Procedure for HEMS and CSMS Agents

Result: Achieve global consensus on energy profiles to satisfy individual objectives and shared objectives (minimize overall energy costs and flatten neighborhood aggregated profile)

Initialization:

- Set initial values for θ, E^H, E^{CS}, $\bar{Z}$, and λ
- Initialize iteration counter $k = 0$

while *dual-residual* $\neq 0$ *or* $k <$ *maximum iterations* **do**

Parallel Update Steps:

- **HEMS Agent:** Update E^H_{k+1} using (23)
- **CSMS Agent:** Update E^{CS}_{k+1} through (24)

Coordinator Update Steps:

- **Global Variable:** Aggregate decisions to form and update average $\bar{Z}_{k+1}$ by (25)
- **Dual Variable:** Update dual variable λ_{k+1} through (26)
- Transmit updated $\bar{Z}$ and λ to all agents for consensus building

Increment iteration counter $k = k + 1$

End:

- Convergence achieved when dual-residual is close to zero (less than the threshold) or maximum iterations reached

4.3. Proposed incentive policy and non-punitive gain allocation

The negotiation between the coordinator and DSO is conducted in a fair and mutually beneficial manner. Assuming successful negotiation, a total incentive function is proposed to determine the DSO's payment to the coordinator for the entire team, proportional to the load factor of the aggregated load profile. Maximizing the daily load factor is selected as an approach to effectively address network constraints. The collective incentive function [1] is formulated as follows,

$$\sigma_{\mathrm{joint}} = \frac{\sigma_{\mathrm{rate}}}{1 + e^{-A(\mathrm{LF}-B)}} \tag{28}$$

The collective incentive rate, denoted as $\sigma_{\mathrm{rate}} = 20\%$, represents the discount applied to the aggregate bill paid to the DSO. This discount can reach a maximum of 20% of the team's aggregated bill. Parameters $A = 20$ and $B = 0.7$ are utilized to adjust the shape of the incentive function. The negotiation between the DSO and coordinator is pivotal in determining the values of σ_{rate}, A, and B. The incentive policy, as presented by (28), offers incentives based on load factors, with no reward for factors at or below 0.4 and a maximum reward of 20% for a factor of 1. Achieving high load factors is challenging due to individual preferences, yet the neighborhood can enhance its load factor, and incentive shares can be distributed based on contributions. The collaboration between HEMSs and CSMS agents forms a coalition aimed at fulfilling individual and joint objectives while maximizing collective gain. Assessing each agent's marginal contribution is crucial for equitable gain allocation, ensuring those who contribute more receive a proportionate share. The gain allocation mechanism is inspired by the Shapley value concept, where the collective gain is allocated based on agents' marginal contributions, promoting fairness and incentivizing active participation in the coordination process.

The coalitional game involves a group of $\mathcal{N}$ agents and a coalition worth function $\mathcal{W}$ that assigns the worth of coalitions to subsets of agents. The share Ψ_i received by agent i in this coalitional game $(\mathcal{W}, C)$ is computed by (29).

$$\Psi_i(\mathcal{W}) = \sum_{C \subseteq \mathbb{C} \setminus \{i\}} \frac{|C|!(\mathcal{N} - |C| - 1)!}{\mathcal{N}!} \mathcal{W}(C \cup \{i\}) - \mathcal{W}(C), \tag{29}$$

$\mathbb{C}$ is the set of all possible agent coalitions, C signifies subsets coalitions, $|C|$ indicates the subset size of C, $\mathcal{W}(C)$ denotes the worth of coalition C, and the sum extends over all subsets C of $\mathbb{C}$ that do not include agent i. The reward-sharing process involves forming all feasible coalitions sequentially, with each agent requesting their fair marginal contribution by (29). The average marginal contribution over feasible permutations is then calculated for each agent. The worth of a coalition C is quantified using $\mathcal{W}$ function defined by (30), ensuring normalization of $\mathcal{W}(C)$ within the range $[0, 1]$. The grand coalition leads to the maximum value of 1.

$$\mathcal{W}(C) = \frac{\left\| E_C^{\mathrm{CR}} - E_C^{\mathrm{NCR}} \right\|_2^2}{\left\| E_{C_G}^{\mathrm{CR}} - E_{C_G}^{\mathrm{NCR}} \right\|_2^2}, \tag{30}$$

In this context, E deputes the coalition's energy profile, C_G stands for the grand coalition of all HEMSs and CSMS agents, E_C^{NCR} describes the energy profile when coalition C does not coordinate, and E_C^{CR} is the profile post-coordination for coalition C. The values $E_{C_G}^{\mathrm{CR}}$ and $E_{C_G}^{\mathrm{NCR}}$ reflects the energy demand for grand coalition C_G after and before coordination, respectively. Eq. (30) ensures that $\mathcal{W}(C)$ remains within the normalized range of 0 to 1. The function $\mathcal{W}(C)$ quantifies how the coalition $C's$ aggregate energy profile adapts to the global variables generated by the coordinator and how much the coalition effort to adapt. This measurement is pivotal for assessing each player's contribution to the coordination and, consequently, determining their shares $(\Psi_i(\mathcal{W}))$ of the collective gain. The proposed non-punitive and Shapley value-based gain sharing mechanism ensures that each agent's reward is directly proportional to its marginal contribution to the overall improvement in the neighborhood's performance without imposing monetary penalties for passive consumers. This contribution is quantified by considering the difference in the collective benefit (primarily measured as improvements in the load factor) achieved with and without that specific agent's participation. In essence, the Shapley value, as illustrated by Eqs. (29) and (30), calculates the average contribution of each agent across all possible coalitions, ensuring a fair distribution of the team's total gain.

Regarding the computational complexity of Shapley values, it is crucial to note that this calculation is part of the billing process, not real-time optimization, making a longer computation time acceptable. In our scenario, the Shapley value calculation typically takes less than one minute. For real-world deployments involving 15–20 houses per local distribution feeder end-transformer, the complexity is manageable. Even for scenarios with more than 20 agents, where a 100% participation factor is unlikely, efficiency can be maintained through estimation approaches to estimate Shapley values with lower computational complexity, for example, by using model agnostic approaches such as Kernel-SHAP or Leverage-SHAP [61,62] or by employing hierarchical coordination framework [63], where agents are divided into smaller groups. This ensures that Shapley value calculations remain efficient and scalable for a large number of consumers.

Table 1
Houses characteristics in the case study.

Location	Thermostats number	Occupants	Area (sq. ft.)	Floors number	Rooms number	Washrooms number	Total rooms	Other
Trois-Rivières	8 to 15	1 to 6	1568 to 4020	up to 2	2 to 5	2 to 4	9 to 15	Spa & Basement.

5. Evaluation framework

This section analyzes the effectiveness of the proposed coordination method for HEMSs and CSMS, presenting the numerical results concisely. The simulations are designed to examine the efficiency of household and EV charging station flexibility. Moreover, the simulations evaluate the adjustments made by households and EV charging stations to their consumption profiles and test the proposed method for distributing the total gain.

5.1. Case study and simulation setup

In this study, we consider a residential neighborhood composed of ten houses, an electric vehicle charging station, and a central neighborhood coordinator. The charging station is equipped with seven EV supply equipment (EVSE) units, each capable of simultaneously charging one EV, allowing for up to seven EVs to be charged at the same time. To ensure the simulation reflects realistic energy usage and charging behavior, the study employs household and load models constructed using real-world data. Specifically, residential consumption profiles are based on datasets from Hydro-Québec for of detached single-family homes located in the city of Trois-Rivières, while EV charging station data is derived from records collected at EVSEs installed on the local university campus. The households use their baseboard heaters as flexible and schedulable assets to participate in the hierarchical coordination program. Table 1 provides a summary of essential parameters for houses, including their location, thermostat count, occupancy, area, and room count. This table offers a comprehensive view of the actual data utilized for consumer modeling. All households are presumed to be equipped with electric baseboard heaters rated at 10 kW. The stochastic consumption profiles and thermal models for households are developed based on empirical data from sources [1,64]. Table 2 provides key EVs' parameters such as the initial and final state of charge ($SOC_{initial}$, SOC_{final}), the arrival time (t_a), the departure time (t_d), rated charging power ($\hat{P}^{v}_{rated}$), charging efficiency ($\hat{\eta}_{c,T}$), battery capacity (Q_{cap}), and EV car models (2023). This data is sourced from the EV database provided by [65]. Each level 2 EVSE has one 1−phase 32A 240 V setup with a maximum charging power of 7.5 kW. Charging efficiency variation with respect to temperature is illustrated in Fig. 4. By exploiting charging records at different temperatures, including parameters such as charging power and state of charge (SOC), an empirical model can be estimated to describe the variation in charging efficiency and duration according to temperature. In fact, these two parameters are significantly impacted in winter charging as illustrated in Fig. 4.

The simulation setup and parameter definitions for the proposed coordination are comprehensively outlined in Table 3. These tables offer a detailed summary of the essential parameters and their values employed in our simulations, ensuring both transparency and reproducibility of the setup. The information provided sheds light on the simulation configuration and the physical and electrical properties pertinent to the case study. Each HEMS agent tackles a convex individual optimization problem using CVXPY coupled with an Embedded Conic Solver (ECOS). The charging station leverages Gekko with the APOPT solver for its optimization tasks. Additionally, the neighborhood coordinator addresses its optimization challenges through CVXPY with an Operator Splitting Quadratic Program (OSQP) solver.

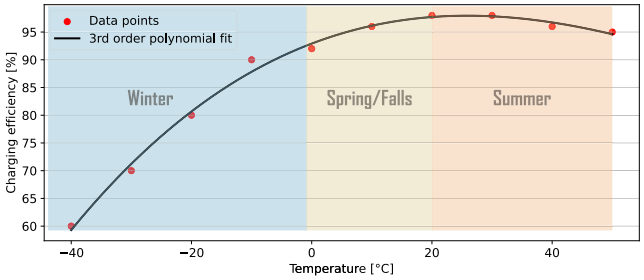

Fig. 4. Charging efficiency variation illustration with respect to the temperature based on the data in [59].

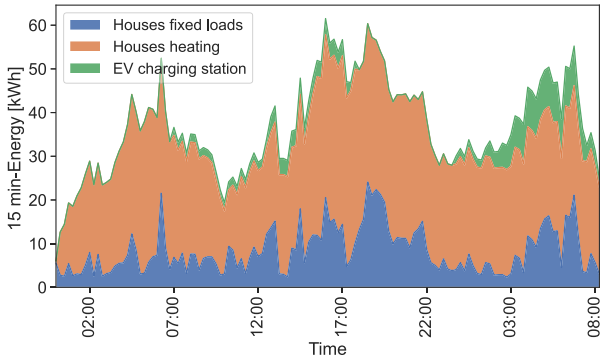

Fig. 5. The baseline scenario highlighting houses and EV charging station consumption profiles.

5.2. Baseline: Without coordination

The baseline scenario outlined in the study excludes dynamic pricing mechanisms and coordinated demand response strategies. In this scenario, each agent (HEMSs and EV station) independently optimizes its electricity costs and meets comfort preferences under a constant daily price of 10 ¢/kWh across all time slots. This approach prioritizes individual objectives, neglecting shared objectives and neighborhood-level coupled constraints. Fig. 5 depicts the baseline consumption profiles of houses, encompassing fixed loads and schedulable loads (electric heaters), and the EV charging station profile. These profiles represent the scenario before any coordination or demand response program implementation. The aggregate neighborhood profile derived from these baselines reveals significant peaks during morning and evening periods. The case studies are set in a winter's cold day context. The objective of the proposed coordination between HEMSs and the EV charging station is to meet consumers' objectives, reduce peak loads in the neighborhood profile (improve load factor), and lower overall energy costs.

5.3. Coordination process and evaluation

This section aims to evaluate the effectiveness of the proposed coordination between HEMSs and the EV charging station within a neighborhood setting. The coordination process involves the neighborhood coordinator negotiating with all agents and sharing updated global variables iteratively, prompting agents to modify their energy

Table 2
Electric Vehicle Parameters [65].

Parameter	EV1	EV2	EV3	EV4	EV5	EV6	EV7
$SOC_{initial}$(%)	25	10	18	35	20	30	11
SOC_{final}(%)	80	82	65	80	70	90	100
t_a (h:mn)	16:00	16:30	17:00	7:30	16:30	17:15	06:30
t_d (h:mn)	7:00 (D+1)	7:30 (D+1)	8:15 (D+1)	17:30	7:30 (D+1)	8:30 (D+1)	18:00
$\hat{P}^{v}_{rated}$(kW)	6.6	7.4	7.4	7.4	7.4	7.4	7.4
$\hat{\eta}_{c,T}$	0.98	0.98	0.98	0.98	0.98	0.98	0.98
$Q_{cap}(kWh)$	40	51	60	71.4	77.4	99.8	111
EVSE type	Level2	Level2	Level2	Level2	Level2	Level2	Level2
Car Model (2023)	Nissan Leaf	Hyundai Kona	Tesla Y	Toyota BZ4X	Hyundai IONIQ5	Kia EV9	Volvo EX90

D+1: designate that this time is for the next day.

Table 3
Simulation setup and parameter definitions for the proposed coordination.

Parameter	cr	ρ	HEMS solver	EV solver	H	$U^{BH,max}$	α [min : max]	β [min : max]	γ [min : max]	θ
Value	1	0.5	CVXPY/OSQP	GEKKO/APOPT	96 (15 min)	10 (kW)	[0.9935 0.9998]	[0.008 0.299]	[0.00028 0.007]	$[10...10]_{1\times96}$

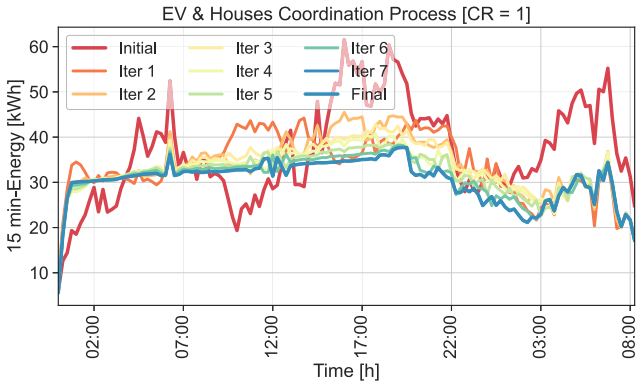

Fig. 6. The iterative coordination to transit and converge from baseline to a global consensus.

consumption profiles. As depicted in Fig. 6, the neighborhood aggregate profile evolves throughout the coordination process, transitioning from the baseline profile (representing the uncoordinated case) to a fully coordinated state where the coordinator optimizes all available flexibility in the neighborhood (CR = 1). The figure demonstrates how agents, including houses and EVs, adjust their profiles to achieve a more flattened aggregate profile (improved load factor), reduce total costs, and meet individual agent preferences and objectives. Additionally, the figure illustrates the progression of the aggregate profile during the coordination process, showcasing its convergence towards the global agreement. Adjusting the convergence rate parameter ρ allows for tuning the convergence speed and influencing how the aggregate profile evolves with each iteration. The outcomes demonstrate a significant enhancement in the load factor by 35%, rising from 0.59 to 0.8. There is a 27% reduction in the total neighborhood discounted bill (after receiving the coordination reward), declining from 119.4 to 87. Moreover, the total neighborhood bill exhibits a 17% reduction prior to the inclusion of coordination rewards and without accounting for discounts, decreasing from 119.4 to 98.8. Additionally, the coordination effectively meets the preferences of EV owners and households alike, aligning with their objectives of comfort and bill minimization.

Fig. 7(a) illustrates the aggregate profile of an EV charging station evolving during the coordination process. The profile transitions from the baseline (uncoordinated case) to a fully coordinated state (CR = 1). The figure shows how the CSMS agent modifies the charging station's profile to contribute to neighborhood coordination. The CSMS agent fulfills all EV car owners' preferences and adheres to their constraints regarding arrival and departure times. Fig. 7(b) highlights the reduction of the EV demand flexibility when a fast charger (level 3) is used

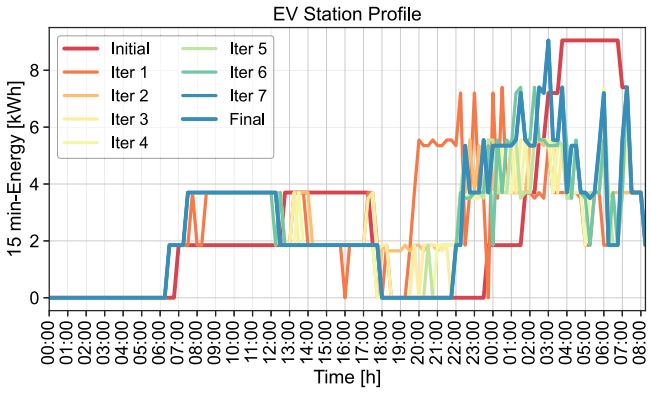

(a) Case of level 2 charging only with more flexibility

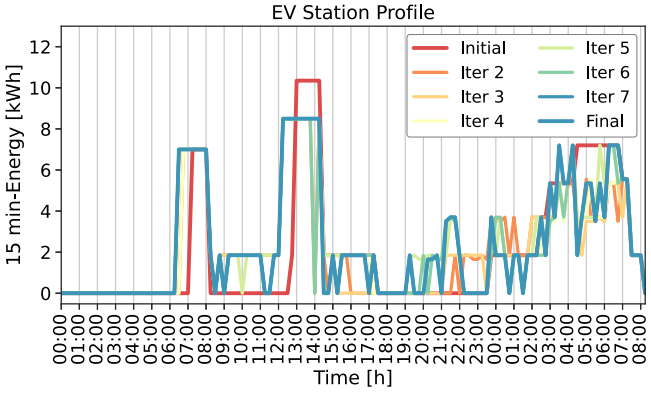

(b) Case of level 2 and 3 charging with less flexibility

Fig. 7. The EV charging station iterative process to transit and converge from baseline to the global consensus.

to charge EVs. In this test, the arrival and departure times, as well as the power rating parameters, were changed to (6:30, 8:15, 28 kW) for EV6 and (12:15, 14:35, 34 kW) for EV7. This result highlights that the more the level 3 chargers are used in place of level 2 chargers, the more the energy demand flexibility of EVs is reduced.

5.4. Coordination level

The section emphasizes the impact of varying the coordination level parameter CR on the coordination outcome and the resulting

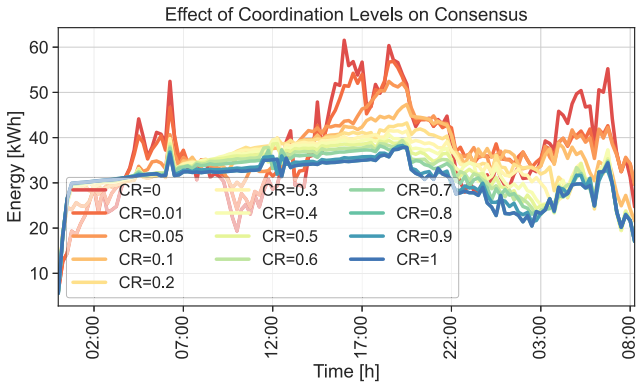

Fig. 8. The effect of coordination level on the global agreement for flattening the aggregate profile and reducing aggregate bill.

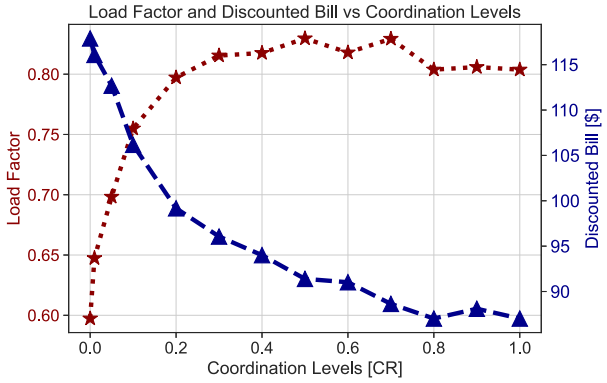

Fig. 9. The effect of coordination level on LF and aggregate bill.

changes in the aggregate profile, load factor, and aggregate bill. Fig. 8 illustrates the aggregate profile of the neighborhood for various levels of coordination within the range of $[0, 1]$. The coordination level parameter CR signifies the relative importance of shared objectives compared to individual objectives. A lower value of CR indicates that agents prioritize individual objectives over common goals. Conversely, a higher value of CR implies that shared objectives are given equal importance as individual goals. The case of $CR = 0$ represents the baseline scenario without coordination, where shared objectives are not prioritized. In contrast, $CR = 1$ represents the maximum coordination level, where shared objectives are as significant as individual objectives. Other coordination levels have been tested and are depicted in the figure.

Fig. 9 illustrates the impact of various coordination levels on the aggregate neighborhood electricity bill (DSO's revenue) and the aggregated consumption profile's load factor (LF). The results indicate that the lowest level of coordination ($CR = 0$) causes the maximum aggregate bill and the minimum LF value, characterized by two significant demand peaks. Consequently, this scenario yields the team's minimum total gain. Conversely, the highest level of coordination ($CR = 1$) achieves the minimum aggregate bill, the maximum LF value with a more flattened profile, and the team's maximum total gain. These findings demonstrate that the coordinator effectively guides the team to satisfy both shared and individual objectives. Higher coordination levels substantially increase the team's gain by improving the LF and reducing the team's total cost.

Fig. 10 demonstrates the relationship between the LF and the reward rate across different coordination levels. The results indicate that as the coordination level increases from $CR = 0$ to $CR = 1$, there is a notable improvement in the aggregated profile's LF. This improvement correlates with an increment in the total team reward rate, illustrating

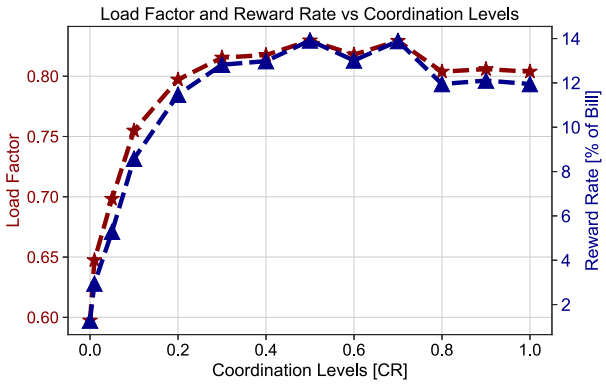

Fig. 10. The effect of coordination level on reward rate and aggregate profile LF.

the positive impact of higher coordination levels on both the efficiency of energy usage and the economic benefits for the team.

5.5. Robustness assessment against model uncertainties

To rigorously assess the robustness and sensitivity of the proposed coordination framework to real-world uncertainties, a comprehensive Monte Carlo simulation was conducted. Four scenarios were evaluated, each isolating or combining key uncertainty sources: EV arrival time (Case 1), departure time (Case 2), initial state of charge (SOC) (Case 3), and all EV parameters combined (Case 4). The uncertainty was modeled by considering variations in EV parameters around their default values which are assumed to be provided by the car owner. Table 4 summarizes the distribution of EV parameters used in the simulation. Each parameter is modeled with a mean and a standard deviation, reflecting realistic variations in EV stochastic parameters. For each scenario, 50 independent simulation runs were performed with $CR = 1$ and $\rho = 1$. In each run, the coordinated load profiles were recorded, and the mean, standard deviation, and corresponding one-standard-deviation error bands (covering 68.2% of outcomes) were computed, as shown in Fig. 11.

The analysis of EV parameter uncertainties reveals that these uncertainties have a limited impact on the aggregated coordinated load profile, as illustrated in Fig. 11. This robustness is primarily due to the predominance of overnight charging in residential contexts, where most EVs are plugged in for extended periods, making the aggregate demand less sensitive to variations in arrival and departure times. While uncertainty in the initial state of charge (SOC) does affect the total energy required, it does not significantly change the overall shape of the load profile. As a result, the coordinated profile remains stable across these scenarios even when combining all EV uncertainties. It is also observed that the variability band is relatively wider during the daytime hours (8:00 to 17:00), reflecting the fact that fewer EVs are scheduled to charge during this period, so individual uncertainties have a more noticeable effect. In contrast, the variability band narrows considerably during the evening and overnight hours (17:00 to 8:00), when most EVs are charging. This leads to a more consistent and predictable aggregate load profile, further demonstrating the inherent robustness of the proposed coordination approach to typical uncertainties in EV charging behavior.

Overall, this comprehensive sensitivity analysis demonstrates that the proposed distributed coordination scheme is robust to a wide range of practical uncertainties, consistently achieving its objectives of peak reduction and cost savings without compromising system stability.

Table 4
Uncertainty parameters for Monte Carlo simulation analysis.

Uncertainty parameter	EV	Mean value	Distribution range	Number of samples
Arrival time (t_a)	EV1	16:00	1h (±30 m)	50
	EV2	16:30	1h (±30 m)	50
	EV3	17:00	1h (±30 m)	50
	EV4	07:30	1h (±30 m)	50
	EV5	16:30	1h (±30 m)	50
	EV6	17:15	1h (±30 m)	50
	EV7	06:30	30 m (±15 m)	50
Departure time (t_d)	EV1	07:00	30 m (±15 m)	50
	EV2	07:30	30 m (±15 m)	50
	EV3	08:15	30 m (±15 m)	50
	EV4	17:30	30 m (±15 m)	50
	EV5	07:30	30 m (±15 m)	50
	EV6	08:15	30 m (±15 m)	50
	EV7	18:00	30 m (±15 m)	50
SOC_0	EV1	25	10 (±5)	50
	EV2	10	5 (±2.5)	50
	EV3	18	5 (±2.5)	50
	EV4	35	10 (±5)	50
	EV5	20	10 (±5)	50
	EV6	30	10 (±5)	50
	EV7	11	5 (±2.5)	50
All parameters	All EVs	Combined	Combined	50

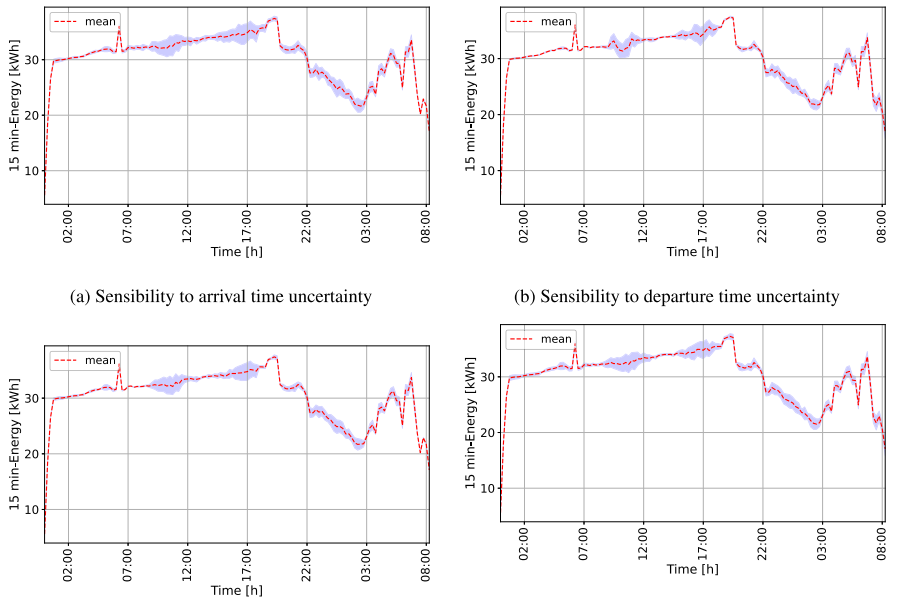

(a) Sensibility to arrival time uncertainty

(b) Sensibility to departure time uncertainty

(c) Sensibility to initial SOC uncertainty

(d) Sensibility to arrival and departure time, and the SOC uncertainty

Fig. 11. Robustness of the proposed method to key EVs parameters uncertainties.

5.6. Consumer contribution and gain sharing

This section evaluates the proposed gain-sharing mechanism designed to measure the contributions of consumers (houses and the EV charging station) in the coordination process. It assesses how effectively the neighborhood's total gain is distributed among participants based on their individual efforts and contributions.

Fig. 12 presents the consumption profiles of consumers before and after implementing the proposed coordination approach, emphasizing each participant's efforts in adjusting their consumption profiles throughout the coordination process. The findings clearly demonstrate different degrees of flexibility among consumers. For example, homes No. 2 and No. 10 exhibit minimal flexibility, while home No. 7 shows the greatest flexibility. The total gain within the neighborhood is allocated to the participants according to their marginal contribution levels (Shapley values), as evidenced by the modification of their profiles during coordination.

As outlined in the reward-sharing mechanism section, calculating each player's contribution level (effort in adjusting its energy profile) to the coordination process is crucial for the fair distribution of the team's total gain. Fig. 12 visually depicts players' contributions, while Fig. 13 showcases the calculated shares allocated to each player through the proposed reward-sharing mechanism. The reward-sharing mechanism (29) divides this total gain among players based on their active engagement in adjusting their consumption profiles during the coordination process. Both active and null participation by players are acceptable. A key aspect of our approach is that while active participants contribute flexibility and are rewarded based on their marginal contribution (effort), null or less active participants receive no additional penalty beyond not receiving a share of the coordination gains, continuing to pay their electricity bills at the standard rate. This gain distribution,

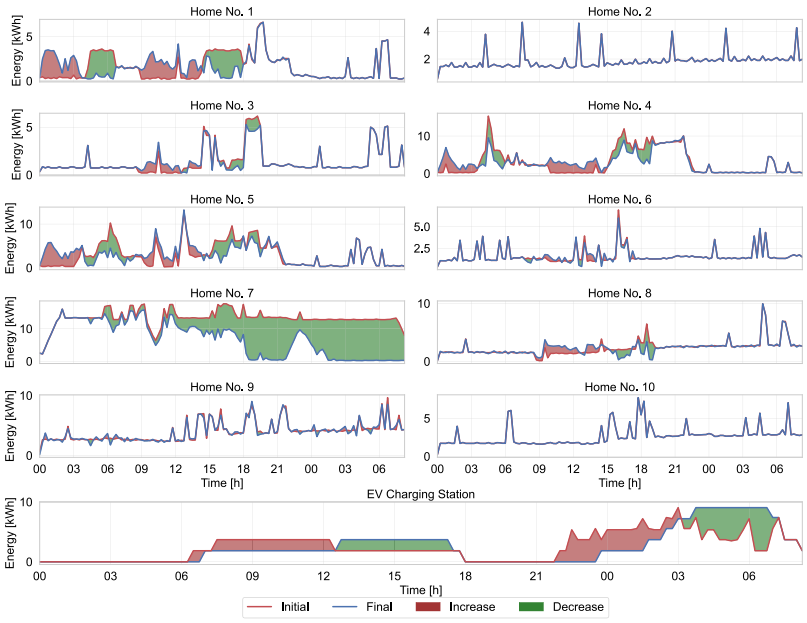

Fig. 12. Consumption profile of consumers after and before DR for CR = 1.

based solely on the marginal contribution of each player to change its daily energy profile, ensures fairness; a player with a higher marginal contribution receives a larger share. Flexibility is allowed, and the level of participation (contribution) for each agent depends on the flexibility effort they are willing to provide. For instance, houses such as No. 2 and No. 10, which demonstrate limited flexibility and minimal interest in coordination, receive no share as they make no effort to adjust their profiles. Conversely, players like No. 1, No. 4, No. 5, No. 7, and the charging station display higher contribution levels and therefore receive larger shares proportionate to their marginal efforts. Each player's share corresponds to its marginal relative contribution to forming the collective effort within the coalition. Adding a strong contributor like consumer No. 7 or the EV charging station to the coalition increases the team's gain, whereas adding a non-contributor like consumer No. 10 has no impact on the team's overall gain. This process ensures that high-contributing players receive higher shares due to their greater marginal contributions.

The coordinator fosters fairness by offering equal opportunities and sharing information transparently with all players, ensuring no superiority among them. Furthermore, the distributed framework ensures robustness and adaptability to changes in neighborhood size and the number of participants; even if some agents choose not to participate or communication is lost, the remaining active agents can continue the coordination process. The aggregation of all players' shares precisely matches the total team's gain, confirming that the intended approach has effectively distributed the entire team's gain among its members in a budget-balanced manner. Fig. 12, therefore, visually represents these participation mechanisms, their impact on coalition dynamics, and the resulting fair reward allocation.

5.7. Comparative analysis

The proposed CSMS and HEMSs coordination strategy is benchmarked against the baseline scenario [66], characterized by individual optimization under a fixed flat pricing mechanism. Additionally, it is evaluated alongside two established indirect coordination methods: dynamic price approach 1 [27] and dynamic price approach 2 [67]. The comparison aimed to showcase the performance of the proposed coordination approach and highlight its superior outcomes in terms of energy efficiency and load factor improvement relative to other methods. The summary of different well-known methods employed for the comparison is as follows:

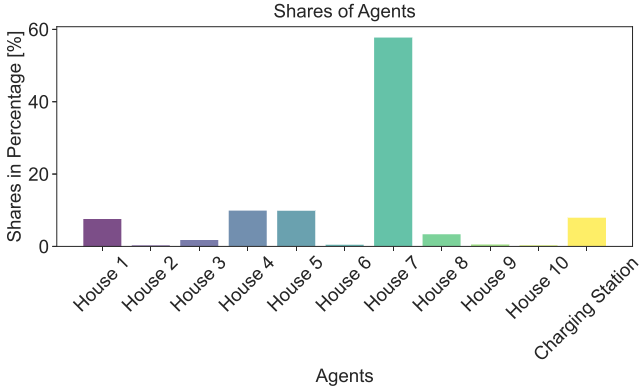

Fig. 13. Shares of agents from the neighborhood's total gain [CR = 1].

Baseline. The baseline scenario [66] represents a situation without using any demand response programs or coordination strategies. Here, each agent independently optimizes to minimize electricity costs under a fixed (flat) daily price profile, ensuring comfort and meeting individual preferences. The flat price is set at 10 ¢/kWh based on [68]. Each agent focuses solely on its own objectives with $\pi = 10$ ¢/kWh, without considering any shared neighborhood's goals.

Proximal dynamic price approach 1. Dynamic Price Approach 1, as per [11,27], implements a negotiated-based pricing mechanism where prices adapt to the aggregate profile of the neighborhood. This approach generates a dynamic day-ahead price profile at the beginning of each day through negotiations between consumers and a neighborhood aggregator. Each agent in the community submits its day-ahead energy demand profile to the aggregator, who aggregates this data to calculate and update the electricity rate. The updated price is then communicated back to consumers, prompting them to adjust their energy demand profiles accordingly. This iterative process continues until the aggregator exhausts all available flexibility in the neighborhood, stabilizing the electricity rate profile. The finalized price profile is established as the price stabilizes across the neighborhood. Mathematically, this dynamic pricing model is represented as $\theta^k = \Gamma * E_N^k$, where $\Gamma = (\theta_0 * E_N).sum()/(E_N * E_N).sum()$, E_N^k denotes the aggregate energy

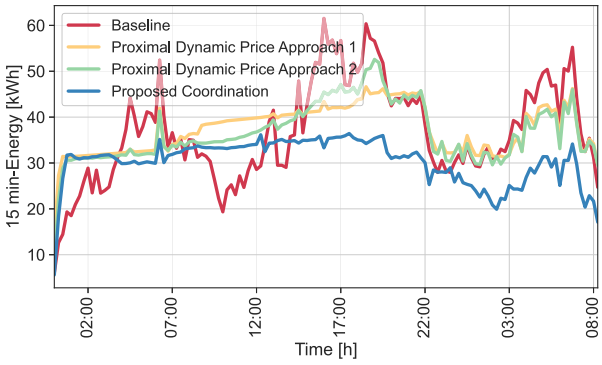

Fig. 14. The comparison of pricing mechanisms across the different scenarios.

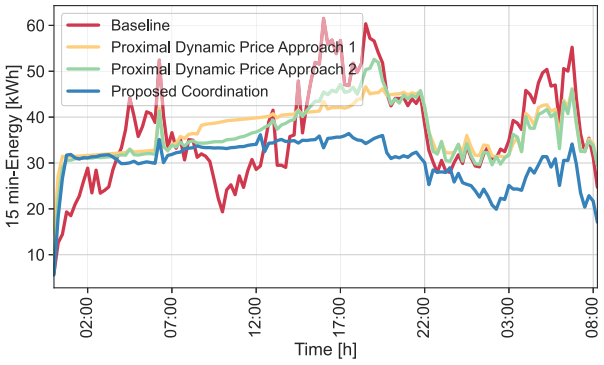

Fig. 15. The comparison of coordination strategies performances and neighborhood aggregate profiles across the four scenarios: (a) baseline, (b) proximal dynamic price 1, (c) proximal dynamic price 2, and (d) our proposed coordination approach.

profile of the neighborhood in iteration k, and θ_0 represents the initial price profile. The coefficient Γ reflects the price elasticity to ensure fluctuations around the desired value, with $\theta_0 = 10$ ¢/kWh according to [68] in this study. In summary, the calculation of Γ normalizes the weights and adjusts θ^k.

Proximal dynamic price approach 2. Dynamic Price Approach 2, based on [67], employs a sophisticated pricing mechanism designed to modulate prices according to the aggregate energy profile of the neighborhood. This approach utilizes a dynamic pricing formula given by $\theta^k[h] = \theta_{min} + (\theta_{\max} - \theta_{min})/(1 + exp(-(E_N^k[h] - M)/\alpha))$, where $\theta^k[h]$ represents the price at time h in iteration k, θ_{min} and $\theta_{\max}$ denote the minimum and maximum price limits, $E_N^k[h]$ signifies the energy demand at time-slot h in iteration k, M represents a reference value for the capacity limitation factor, and α controls the rate of change of the price function (smoothness). The design of this pricing formula incorporates a sigmoid function, leveraging mathematical properties to adjust prices dynamically based on energy demand fluctuations. The sigmoid function ensures that prices respond sensibly to changes in energy demand, with a gradual increase or decrease in prices as energy demand deviates from the reference value $M = 30$. This design aims to encourage consumers to shift their energy consumption patterns in response to price variations, promoting energy efficiency and load management within the neighborhood. In summary, Dynamic Price Approach 2 employs a sigmoid-based pricing model that adapts prices flexibly to the energy demand profile, fostering efficient energy utilization and load balancing across the community.

5.7.1. Electricity price profiles

The difference between the electricity price profiles in different approaches is clarified in Fig. 14. In our proposed neighborhood's HEMSs and EV charging station coordination, a fixed flat price mechanism is utilized to ensure fairness among all consumers regarding the shifting of their energy consumption. This approach prevents consumer complaints about unequal pricing, as it ensures that no consumer benefits from lower prices while others face higher prices. By maintaining a consistent price, all consumers are treated equally, promoting fairness in the distribution of energy costs and consumption shifts. Conversely, the other two pricing mechanisms generate the price signal based on energy demand in each time-slot or according to peak-shaving objectives, as detailed in the sections on Dynamic Price Approach 1 and Dynamic Price Approach 2. These dynamic approaches adjust prices in response to demand fluctuations or peak load objectives, aiming to penalize consumers for consuming during peak times, thereby encouraging them to shift their energy usage to off-peak periods, which helps to optimize the overall load profile.

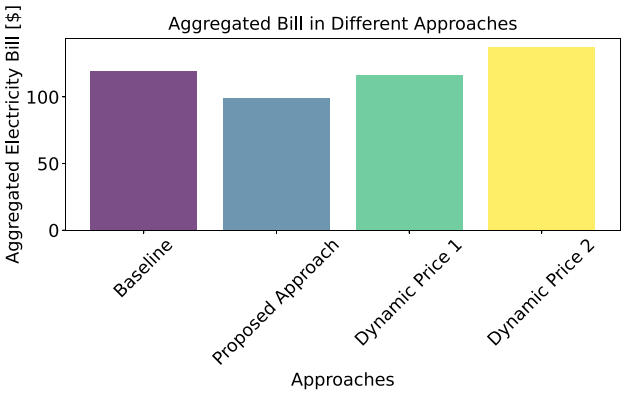

Fig. 16. The comparison of aggregate bills across the four scenarios.

5.7.2. Coordination performance

This section aims to compare the effectiveness of the proposed coordination between HEMSs and the CSMS within the neighborhood with three different approaches. Fig. 15 compares the neighborhood aggregate energy profile in four scenarios: (a) baseline, (b) proposed approach (with CR = 1), (c) dynamic price 1, and (d) dynamic price 2.

The comparison demonstrates a significant improvement in the load factor by using our proposed coordination approach, increasing by up to 35% compared with the baseline scenario, from 0.59 to 0.8. Besides, it reduces the total neighborhood discounted bill up to 27%, decreasing from 119.4 to 87. The proposed coordination effectively fulfills both common objectives (aggregate profile flatness and aggregate bill reduction) and individual objectives (such as the bill minimization and comfort preferences of EV owners and households). A detailed comparison of the neighborhood's total energy cost reduction and the neighborhood aggregate profile load factor improvement in the four different approaches is presented in Fig. 16 and Fig. 17, respectively. The results in the figures Figs. 16 and 17 highlight that the proposed coordination approach, compared to other approaches, achieves the lowest neighborhood aggregate bill (indicating the highest energy efficiency) and the highest load factor (indicating the most flattened profile).

5.8. Practical implementation of proposed coordination framework

The proposed distributed coordination framework is designed for practical, scalable, and cost-effective implementation in real-world residential environments. Its distributed architecture, based on the ADMM algorithm, enables seamless addition or removal of agents (HEMSs and

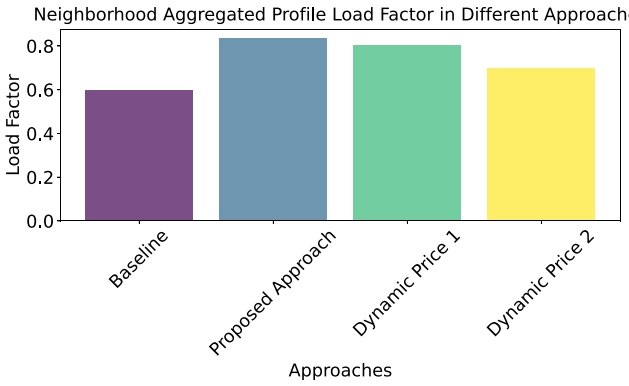

Fig. 17. The comparison of aggregate profile load factor across the four scenarios.

CSMSs) without system reconfiguration, making it inherently adaptable to neighborhoods of varying sizes. By decomposing the global optimization problem into smaller, parallel subproblems for each agent, the framework efficiently manages computational complexity, preserves privacy, and supports real-time operation. Each agent solves a convex optimization problem of limited size, which can be handled by open-source solvers such as CVXPY or Gekko on low-cost edge devices (e.g., Raspberry Pi), minimizing hardware costs. The framework's asynchronous and distributed nature ensures resilience to communication disruptions, allowing agents to operate locally and re-synchronize when connectivity is restored.

Communication between agents leverages lightweight, widely adop ted protocols such as WebSocket, MQTT, or Zigbee, which are already prevalent in smart appliances and commercial EVSEs. This facilitates integration with existing residential infrastructure and reduces the need for extensive hardware upgrades. The central coordinator can be flexibly hosted either on cloud platforms or local edge servers. Furthermore, the increasing market penetration of smart appliances (e.g., Tasmota, Shelly, Hydro-Québec Hilo and Mysa Smart Thermostats, etc.) further supports practical feasibility.

For the incentive mechanism, Shapley value calculations are performed at the distribution transformer (neighborhood) level, where the number of agents is typically limited and manageable. For larger-scale scenarios, hierarchical approaches can be employed to maintain computational feasibility [63]. In this setup, local coordinators (representing neighborhoods groups) compute Shapley values for their respective agents, and these results are then aggregated at higher levels (e.g., at the distribution transformer). To further reduce computational complexity for very large populations, efficient estimation techniques such as Kernel SHAP or Leverage SHAP can be applied [61,62]. This hierarchical structure keeps computations tractable while ensuring fair and transparent incentive allocation across all agents.

The framework's asynchronous and distributed nature ensures resilience to communication disruptions, allowing agents to operate locally and re-synchronize when connectivity is restored. While the computational demands and communication overhead are minimized by design, practical deployment must still address challenges such as uncertainty in user behavior, flexibility estimation, communication reliability, and the availability of real-time data to further demonstrate the framework's effectiveness.

While the computational demands and communication overhead are minimized by design, practical deployment must still address challenges such as uncertainties through stochastic decision mechanism, flexibility estimation, communication reliability, and the availability of real-time data to further demonstrate the framework's effectiveness. Future work should focus on field testing to validate the framework under real-world conditions. These efforts should also address infrastructure costs, communication and control constraints, and support the full-scale deployment of the proposed coordination system in residential neighborhoods.

6. Conclusion

This paper addressed the challenges posed by uncoordinated electric vehicles Charging Station Management Systems (CSMS) and Home Energy Management Systems (HEMSs) in distribution networks, resulting in increased power loss and the creation of demand peaks. The paper proposed a distributed coordination approach to manage CSMS and HEMSs, aiming to mitigate these negative impacts within a neighborhood setting. The approach explicitly modeled consumer flexibility, considering users' energy demand, preferences, and CSMS features such as EV arrival/departure times, state of charge, and scheduling energy requirements. CSMS and HEMS Agents make rational decisions based on limited information. The coordination technique not only meets individual CSMS and HEMS objectives but also addresses shared neighborhood objectives. Shared objectives are distributed among agents to guide optimal complementary decision-making processes. The proposed framework is modular and scalable, allowing seamless integration of new flexible loads (e.g., heat pumps, smart appliances) and adaptation to neighborhoods of varying sizes. Its distributed architecture ensures practical deployment using existing smart devices and low-cost controllers, while maintaining privacy and resilience to communication disruptions. The method sought to align HEMS and CSMS consumption profiles to smoother aggregated profiles and lower overall energy costs. An incentive allocation mechanism has been devised to evaluate agents' marginal contributions and distribute rewards accordingly. Case studies assessed the proposed coordination across diverse preferences and coordination levels, comparing it with uncoordinated (baseline) and indirectly coordinated (proximal dynamic price) scenarios. Key outcomes include improved consumers' load profile alignment, reduced energy costs, and fair reward distribution based on their contributions. The proposed neighborhood coordination resulted in a significant improvement in the neighborhood aggregate profile's load factor, increasing by up to 35% from 0.59 to 0.8. Additionally, it led to a reduction of up to 27% in the total neighborhood discounted bill, decreasing from 119.4 to 87. The proposed distributed coordination framework also demonstrated robustness to typical uncertainties in EV charging behavior, maintaining stable aggregate profiles even under variations in arrival/departure times and state of charge.

CRediT authorship contribution statement

Farshad Etedadi: Writing – review & editing, Writing – original draft, Validation, Software, Methodology, Conceptualization. **Abdoul Wahab Danté:** Writing – review & editing, Writing – original draft, Methodology, Conceptualization. **Sousso Kelouwani:** Writing – review & editing, Supervision, Project administration. **Nilson Henao:** Writing – review & editing, Supervision, Data curation. **Kodjo Agbossou:** Writing – review & editing, Supervision, Project administration, Funding acquisition. **Michaël Fournier:** Writing – review & editing, Supervision.

Declaration of competing interest

The authors declare the following financial interests/personal relationships which may be considered as potential competing interests: Farshad Etedadi reports was provided by University of Quebec at Trois-Rivieres. If there are other authors, they declare that they have no known competing financial interests or personal relationships that could have appeared to influence the work reported in this paper.

Acknowledgments

This work was supported in part by the Laboratoire des technologies de l'energie (LTE) d'Hydro-Quebec, the Natural Science and Engineering Research Council of Canada and the Fondation of UQTR.

Data availability

The data that has been used is confidential.

References

[1] Etedadi F, Kelouwani S, Agbossou K, Henao N, Laurencelle F. Consensus and sharing based distributed coordination of home energy management systems with demand response enabled baseboard heaters. Appl Energy 2023;336:120833. http://dx.doi.org/10.1016/j.apenergy.2023.120833, URL: https://linkinghub.elsevier.com/retrieve/pii/S0306261923001976.

[2] Etedadi F, Agbossou K, Kelouwani S, Henao N, Hosseini S. Coordination of smart home energy management systems in neighborhood areas: A systematic review. IEEE Access 2021;9:36417–43. http://dx.doi.org/10.1109/ACCESS.2021.3061995, URL: https://ieeexplore.ieee.org/document/9363112/.

[3] Khalid A, Javaid N, Guizani M, Alhussein M, Aurangzeb K, Ilahi M. Towards dynamic coordination among home appliances using multi-objective energy optimization for demand side management in smart buildings. IEEE Access 2018;6:19509–29. http://dx.doi.org/10.1109/ACCESS.2018.2791546.

[4] Anvari-Moghaddam A, Rahimi-Kian A, Mirian MS, Guerrero JM. A multi-agent based energy management solution for integrated buildings and microgrid system. Appl Energy 2017;203:41–56. http://dx.doi.org/10.1016/j.apenergy.2017.06.007.

[5] Cheng Z, Li Z, Liang J, Si J, Dong L, Gao J. Distributed coordination control strategy for multiple residential solar PV systems in distribution networks. Int J Electr Power Energy Syst 2020;117:105660. http://dx.doi.org/10.1016/j.ijepes.2019.105660.

[6] Bahrami S, Amini MH. A decentralized trading algorithm for an electricity market with generation uncertainty. Appl Energy 2018;218:520–32. http://dx.doi.org/10.1016/j.apenergy.2018.02.157, URL: https://linkinghub.elsevier.com/retrieve/pii/S0306261918302915.

[7] Zhang N, Yan Y, Su W. A game-theoretic economic operation of residential distribution system with high participation of distributed electricity prosumers. Appl Energy 2015;154:471–9. http://dx.doi.org/10.1016/j.apenergy.2015.05.011.

[8] Langenmayr U, Wang W, Jochem P. Unit commitment of photovoltaic-battery systems: An advanced approach considering uncertainties from load, electric vehicles, and photovoltaic. Appl Energy 2020;280:115972. http://dx.doi.org/10.1016/J.APENERGY.2020.115972.

[9] Yi Z, Scoffield D, Smart J, Meintz A, Jun M, Mohanpurkar M, Medam A. A highly efficient control framework for centralized residential charging coordination of large electric vehicle populations. Int J Electr Power Energy Syst 2020;117:105661. http://dx.doi.org/10.1016/j.ijepes.2019.105661, URL: https://linkinghub.elsevier.com/retrieve/pii/S0142061519321775.

[10] Li Z, Ma C. A temporal–spatial charging coordination scheme incorporating probability of EV charging availability. Appl Energy 2022;325:119838. http://dx.doi.org/10.1016/J.APENERGY.2022.119838, URL: https://linkinghub.elsevier.com/retrieve/pii/S0306261922011072.

[11] Etedadi F, Agbossou K, Henao N, Kelouwani S, Laurencelle F. Distributed residential demand response using building mass and electric thermal storage system. In: 2022 IEEE 10th international conference on smart energy grid engineering. Oshawa, Canada: IEEE; 2022, p. 19–25. http://dx.doi.org/10.1109/SEGE55279.2022.9889758, URL: https://ieeexplore.ieee.org/document/9889758/.

[12] Kersic M, Bocklisch T, Böttiger M, Gerlach L. Coordination mechanism for PV battery systems with local optimizing energy management. Energies 2020;13(3):611. http://dx.doi.org/10.3390/en13030611, URL: https://www.mdpi.com/1996-1073/13/3/611.

[13] Exploring Canada's Energy Future - Canada Energy Regulator, [https://bit.ly/3qGE2bW].

[14] An updated roadmap to Net Zero Emissions by 2050 – World Energy Outlook 2022 – Analysis - IEA, https://www.iea.org/reports/world-energy-outlook-2022/an-updated-roadmap-to-net-zero-emissions-by-2050.

[15] Dante AW, Kelouwani S, Agbossou K, Henao N, Bouchard J, Hosseini SS. A stochastic approach to designing plug-in electric vehicle charging controller for residential applications. IEEE Access 2022;10:52876–89. http://dx.doi.org/10.1109/ACCESS.2022.3175817.

[16] Abdelaal G, Gilany MI, Elshahed M, Sharaf HM, El'gharably A. Integration of electric vehicles in home energy management considering urgent charging and battery degradation. IEEE Access 2021;9:47713–30. http://dx.doi.org/10.1109/ACCESS.2021.3068421.

[17] Khemakhem S, Rekik M, Krichen L. A power management strategy for a wind energy conversion system and plug-in electric vehicles in residential applications. In: Hirech K, editor. Pioneering sustainable innovations in renewable energy technologies. Hershey, PA, USA: IGI Global Scientific Publishing; 2025, p. 147–72. http://dx.doi.org/10.4018/979-8-3693-9924-8.ch008, URL: https://services.igi-global.com/resolvedoi/resolve.aspx?doi=10.4018/979-8-3693-9924-8.ch008.

[18] Ben Arab M, Rekik M, Krichen L. Suitable various-goal energy management system for smart home based on photovoltaic generator and electric vehicles. J Build Eng 2022;52:104430. http://dx.doi.org/10.1016/j.jobe.2022.104430, URL: https://www.sciencedirect.com/science/article/pii/S2352710222004430.

[19] Smaoui M, Rekik M, Krichen L. Optimal design of an off-grid electrical system in remote areas with different renewable energy scenarios. Energy 2025;318:134821. http://dx.doi.org/10.1016/j.energy.2025.134821, URL: https://www.sciencedirect.com/science/article/pii/S0360544225004633.

[20] Sagaria S, van der Kam M, Boström T. Vehicle-to-grid impact on battery degradation and estimation of V2g economic compensation. Appl Energy 2025;377:124546. http://dx.doi.org/10.1016/j.apenergy.2024.124546, URL: https://www.sciencedirect.com/science/article/pii/S0306261924019299.

[21] Fachrizal R, Ramadhani UH, Munkhammar J, Widén J. Combined PV–EV hosting capacity assessment for a residential LV distribution grid with smart EV charging and PV curtailment. Sustain Energy Grids Netw 2021;26:100445. http://dx.doi.org/10.1016/j.segan.2021.100445, URL: https://www.sciencedirect.com/science/article/pii/S2352467721000163.

[22] Sarmokadam S, Suresh M, Mathew R. Power flow control strategy for prosumer based EV charging scheme to minimize charging impact on distribution network. Energy Rep 2025;13:3794–809. http://dx.doi.org/10.1016/j.egyr.2025.03.032, URL: https://www.sciencedirect.com/science/article/pii/S2352484725001726.

[23] Liu N, Yu X, Wang C, Wang J. Energy sharing management for microgrids with PV prosumers: A stackelberg game approach. IEEE Trans Ind Inform 2017;13(3):1088–98. http://dx.doi.org/10.1109/TII.2017.2654302.

[24] Jia L, Tong L. Dynamic pricing and distributed energy management for demand response. IEEE Trans Smart Grid 2016;7(2):1128–36. http://dx.doi.org/10.1109/TSG.2016.2515641, arXiv:1601.02319.

[25] Adika CO, Wang L. Non-cooperative decentralized charging of homogeneous households' batteries in a smart grid. IEEE Trans Smart Grid 2014;5(4):1855–63. http://dx.doi.org/10.1109/TSG.2014.2302449.

[26] Safdarian A, Fotuhi-Firuzabad M, Lehtonen M. Optimal residential load management in smart grids: A decentralized framework. IEEE Trans Smart Grid 2016;7(4):1836–45. http://dx.doi.org/10.1109/TSG.2015.2459753, URL: http://ieeexplore.ieee.org/document/7202880/.

[27] Celik B, Roche R, Bouquain D, Miraoui A. Decentralized neighborhood energy management with coordinated smart home energy sharing. IEEE Trans Smart Grid 2018;9(6):6387–97. http://dx.doi.org/10.1109/TSG.2017.2710358, URL: https://ieeexplore.ieee.org/document/7937821/.

[28] Mak D, Choi DH. Optimization framework for coordinated operation of home energy management system and volt-VAR optimization in unbalanced active distribution networks considering uncertainties. Appl Energy 2020;276:115495. http://dx.doi.org/10.1016/j.apenergy.2020.115495.

[29] Wu X, Hu X, Yin X, Moura SJ. Stochastic optimal energy management of smart home with PEV energy storage. IEEE Trans Smart Grid 2018;9(3):2065–75. http://dx.doi.org/10.1109/TSG.2016.2606442, URL: https://ieeexplore.ieee.org/document/7562357/.

[30] Li J, Li C, Xu Y, Dong ZY, Wong KP, Huang T. Noncooperative game-based distributed charging control for plug-in electric vehicles in distribution networks. IEEE Trans Ind Inform 2018;14(1):301–10. http://dx.doi.org/10.1109/TII.2016.2632761.

[31] liu z, Wu Q, Shahidehpour M, Li C, Huang S, Wei W. Transactive real-time electric vehicle charging management for commercial buildings with PV on-site generation. IEEE Trans Smart Grid 2019;10(5):4939–50. http://dx.doi.org/10.1109/TSG.2018.2871171, URL: https://ieeexplore.ieee.org/document/8467995/.

[32] Tushar MHK, Assi C, Maier M, Uddin MF. Smart microgrids: Optimal joint scheduling for electric vehicles and home appliances. IEEE Trans Smart Grid 2014;5(1):239–50. http://dx.doi.org/10.1109/TSG.2013.2290894.

[33] de Souza Dutra MD, Alguacil N. Optimal residential users coordination via demand response: An exact distributed framework. Appl Energy 2020;279:115851. http://dx.doi.org/10.1016/J.APENERGY.2020.115851.

[34] Dong L, Wu Q, Hong J, Wang Z, Fan S, He G. An adaptive decentralized regulation strategy for the cluster with massive inverter air conditionings. Appl Energy 2023;330:120304. http://dx.doi.org/10.1016/J.APENERGY.2022.120304.

[35] Zhang Z, Deng R, Yuan T, Joe Qin S. Bi-level demand response game with information sharing among consumers. IFAC-PapersOnLine 2016;49(7):663–8. http://dx.doi.org/10.1016/j.ifacol.2016.07.252, URL: https://linkinghub.elsevier.com/retrieve/pii/S2405896316304591.

[36] Han L, Morstyn T, McCulloch M. Incentivizing prosumer coalitions with energy management using cooperative game theory. IEEE Trans Power Syst 2019;34(1):303–13. http://dx.doi.org/10.1109/TPWRS.2018.2858540, URL: https://ieeexplore.ieee.org/document/8417894/.

[37] Juelsgaard M, Andersen P, Wisniewski R. Distribution loss reduction by household consumption coordination in smart grids. IEEE Trans Smart Grid 2014;5(4):2133–44. http://dx.doi.org/10.1109/TSG.2014.2312428.

[38] Zhang J, Che L, Wan X, Shahidehpour M. Distributed hierarchical coordination of networked charging stations based on peer-to-peer trading and EV charging flexibility quantification. IEEE Trans Power Syst 2022;37(4):2961–75. http://dx.doi.org/10.1109/TPWRS.2021.3123351.

[39] Chen N, Tan CW, Quek TQ. Electric vehicle charging in smart grid: Optimality and valley-filling algorithms. IEEE J Sel Top Signal Process 2014;8(6):1073–83. http://dx.doi.org/10.1109/JSTSP.2014.2334275.

[40] Liu M, Phanivong PK, Shi Y, Callaway DS. Decentralized charging control of electric vehicles in residential distribution networks. IEEE Trans Control Syst Technol 2019;27(1):266–81. http://dx.doi.org/10.1109/TCST.2017.2771307, arXiv:1710.05533.

[41] Kumar Nunna HS, Battula S, Doolla S, Srinivasan D. Energy management in smart distribution systems with vehicle-to-grid integrated microgrids. IEEE Trans Smart Grid 2018;9(5):4004–16. http://dx.doi.org/10.1109/TSG.2016.2646779.

[42] Oshnoei A, Kheradmandi M, Muyeen SM. Robust control scheme for distributed battery energy storage systems in load frequency control. IEEE Trans Power Syst 2020;35(6):4781–91. http://dx.doi.org/10.1109/TPWRS.2020.2997950.

[43] Chaudhari K, Kandasamy NK, Krishnan A, Ukil A, Gooi HB. Agent-based aggregated behavior modeling for electric vehicle charging load. IEEE Trans Ind Inform 2019;15(2):856–68. http://dx.doi.org/10.1109/TII.2018.2823321.

[44] Wang B, Dehghanian P, Zhao D. Chance-constrained energy management system for power grids with high proliferation of renewables and electric vehicles. IEEE Trans Smart Grid 2020;11(3):2324–36. http://dx.doi.org/10.1109/TSG.2019.2951797.

[45] Fan H, Duan C, Zhang CK, Jiang L, Mao C, Wang D. ADMM-based multi-period optimal power flow considering plug-in electric vehicles charging. IEEE Trans Power Syst 2018;33(4):3886–97. http://dx.doi.org/10.1109/TPWRS.2017.2784564.

[46] Zhou X, Zou S, Wang P, Ma Z. Voltage regulation in constrained distribution networks by coordinating electric vehicle charging based on hierarchical ADMM. IET Gener Transm Distrib 2020;14(17):3444–57. http://dx.doi.org/10.1049/IET-GTD.2020.0415.

[47] Chen L, Yu T, Chen Y, Guan W, Shi Y, Pan Z. Real-time optimal scheduling of large-scale electric vehicles: A dynamic non-cooperative game approach. IEEE Access 2020;8:133633–44. http://dx.doi.org/10.1109/ACCESS.2020.3009039.

[48] Rahman T, Xu Y, Qu Z. Continuous-domain real-time distributed ADMM algorithm for aggregator scheduling and voltage stability in distribution network. IEEE Trans Autom Sci Eng 2022;19(1):60–9. http://dx.doi.org/10.1109/TASE.2021.3072932.

[49] Khalid MR, Alam MS, Sarwar A, Asghar MSJ. A comprehensive review on electric vehicles charging infrastructures and their impacts on power-quality of the utility grid. ETransportation 2019;1:100006. http://dx.doi.org/10.1016/J.ETRAN.2019.100006.

[50] Unterluggauer T, Rich J, Andersen PB, Hashemi S. Electric vehicle charging infrastructure planning for integrated transportation and power distribution networks: A review. ETransportation 2022;12:100163. http://dx.doi.org/10.1016/J.ETRAN.2022.100163.

[51] Li N, Chen L, Low SH. Optimal demand response based on utility maximization in power networks. In: IEEE Power and Energy Society General Meeting. 2011, http://dx.doi.org/10.1109/PES.2011.6039082.

[52] Castillo L, Enríquez R, Jiménez MJ, Heras MR. Dynamic integrated method based on regression and averages, applied to estimate the thermal parameters of a room in an occupied office building in madrid. Energy Build 2014;81:337–62. http://dx.doi.org/10.1016/J.ENBUILD.2014.06.039.

[53] Wani M, Hafiz F, Swain A, Ukil A. Estimating thermal parameters of a commercial building: A meta-heuristic approach. Energy Build 2021;231:110537. http://dx.doi.org/10.1016/J.ENBUILD.2020.110537.

[54] Sharma G, Sood VK, Alam MS, Shariff SM. Comparison of common DC and AC bus architectures for EV fast charging stations and impact on power quality. ETransportation 2020;5:100066. http://dx.doi.org/10.1016/J.ETRAN.2020.100066.

[55] Bilfinger P, Rosner P, Schreiber M, Kröger T, Gamra KA, Ank M, Wassiliadis N, Dietermann B, Lienkamp M. Battery pack diagnostics for electric vehicles: Transfer of differential voltage and incremental capacity analysis from cell to vehicle level. ETransportation 2024;22:100356. http://dx.doi.org/10.1016/J.ETRAN.2024.100356.

[56] Zhang YZ, Xiong R, He HW, Qu X, Pecht M. Aging characteristics-based health diagnosis and remaining useful life prognostics for lithium-ion batteries. ETransportation 2019;1:100004. http://dx.doi.org/10.1016/J.ETRAN.2019.100004.

[57] Danté AW, Agbossou K, Kelouwani S, Cardenas A, Bouchard J. Online modeling and identification of plug-in electric vehicles sharing a residential station. Int J Electr Power Energy Syst 2019;108:162–76. http://dx.doi.org/10.1016/j.ijepes.2018.12.024.

[58] Qian K, Zhou C, Allan M, Yuan Y. Modeling of load demand due to EV battery charging in distribution systems. IEEE Trans Power Syst 2011;26(2):802–10. http://dx.doi.org/10.1109/TPWRS.2010.2057456.

[59] Lv S, Wang X, Lu W, Zhang J, Ni H. The influence of temperature on the capacity of lithium ion batteries with different anodes. Energies 2021;15:60. http://dx.doi.org/10.3390/EN15010060, https://www.mdpi.com/1996-1073/15/1/60/htm https://www.mdpi.com/1996-1073/15/1/60.

[60] Han X, Lu L, Zheng Y, Feng X, Li Z, Li J, Ouyang M. A review on the key issues of the lithium ion battery degradation among the whole life cycle. ETransportation 2019;1:100005. http://dx.doi.org/10.1016/J.ETRAN.2019.100005.

[61] Musco C, Witter RT. Provably accurate Shapley value estimation via leverage score sampling. 2024, arXiv preprint arXiv:2410.01917.

[62] Chen H, Covert IC, Lundberg SM, Lee S-I. Algorithms to estimate Shapley value feature attributions. Nat Mach Intell 2023;5(6):590–601. http://dx.doi.org/10.1038/s42256-023-00657-x.

[63] Etedadi F, Kelouwani S, Agbossou K, Henao N, Laurencelle F, Hosseini SS. Hierarchical transactive home energy management system groups coordination through multi-level consensus sharing-based distributed ADMM. Sustain Energy Grids Netw 2024;39:101460. http://dx.doi.org/10.1016/j.segan.2024.101460, URL: https://www.sciencedirect.com/science/article/pii/S2352467724001899.

[64] Henao N, Fournier M, Kelouwani S, De T. Characterizing smart thermostats operation in residential zoned heating systems and its impact on energy saving metrics of electrical and computer engineering of universit ' e du qu ' ebec a ebec , Canada institut de recherche d ' hydro-qu ' ebec , Canada. In: Proceedings of eSim 2018, the 10th conference of IBPSA-Canada. 2018.

[65] EV-Database. Useable battery capacity of full electric vehicles cheatsheet - EV Database, URL: https://ev-database.org/cheatsheet/useable-battery-capacity-electric-car.

[66] Vardakas JS, Zorba N, Verikoukis CV. A survey on demand response programs in smart grids: Pricing methods and optimization algorithms. IEEE Commun Surv Tutor 2015;17(1):152–78. http://dx.doi.org/10.1109/COMST.2014.2341586.

[67] Fraija A, Henao N, Agbossou K, Kelouwani S, Fournier M, Nagarsheth SH. Deep reinforcement learning based dynamic pricing for demand response considering market and supply constraints. Smart Energy 2024;14:100139. http://dx.doi.org/10.1016/J.SEGY.2024.100139.

[68] Rate D | hydro-québec. 2022, URL: https://www.hydroquebec.com/residential/customer-space/rates/rate-d.html. [Accessed 02 January 2022].